AN INVESTIGATION OF MOLECULAR MOTION IN STEARIC ACID BY PROTON MAGNETIC RESONANCE

by

THEODORE J.R. CYR

B.Sc., The University of British Columbia, 1963

A THESIS SUBMITTED IN PARTIAL FULFILMENT OF
THE REQUIREMENTS FOR THE DEGREE OF

Master of Science

in the Department

of

CHEMISTRY

We accept this thesis as conforming to the

required standard

THE UNIVERSITY OF BRITISH COLUMBIA

January, 1966

In presenting this thesis in partial fulfilment of the requirements for an advanced degree at the University of British Columbia, I agree that the Library shall make it freely available for reference and study. I further agree that permission for extensive copying of this thesis for scholarly purposes may be granted by the Head of my Department or by his representatives. It is understood that copying or publication of this thesis for financial gain shall not be allowed without my written permission.

Department of Chemistry

The University of British Columbia,
Vancouver 8, Canada

Date January 18, 1966

ABSTRACT

The proton magnetic resonance absorption of the C-form of stearic acid has been studied over the temperature range 77°K to 342.5°K.

The broadline spectra are decomposed into a wide and narrow component for solid and liquid regions in the lattice respectively. The appearance of the narrow component on the usual broadline spectrum at temperatures greater than room temperature is interpreted to be caused by large liquid regions in the lattice. The number and size of these defects increase with increase in temperature and with the incorporation of various types of defects in the solid lattice

The spin-lattice relaxation times, T_1, were measured by adiabatic rapid passage. The results indicate that the principal zeeman energy-thermal bath coupling occurs through methyl group reorientations. An activation energy of 2.2 kcalories/mole for methyl group rotation about the C_3 axis in solid stearic acid and a rotation frequency of 4×10^5 sec^{-1} at 77°K were determined from the T_1 data.

ACKNOWLEDGMENTS

The writing of this thesis has been made an interesting and informative persuit through the consultation and advice of my thesis advisor, Professor B. A. Dunell. Professor B. A. Dunell deserves special commendation for his gifts of encouragement, direction and general personal attention during the entire project.

Indebtedness is also to be expressed to Mr. W. R. Janzen who helped in the repairing of the NMR equipment which was subject to continual and unpredictable breakdown.

Professor B. A. Dunell gave invaluable aid by cooperating to bring this work into an asthetically pleasing and acceptable form. The final draft of the thesis was typed by Miss L. C. Liu.

Completion of the project has been made possible through funds derived from the National Research Council of Canada and the Department of Chemistry at U.B.C.

TABLE OF CONTENTS

List of Figures

INTRODUCTION

Solid stearic acid can be classified as a crystalline substance. A properly defined melting temperature exists for the substance. At this temperature, equilibrium between the crystalline and liquid phases can be established. A first-order phase transition characterizes the fusion, and the melting temperature is systematically depressed by the addition of impurities according to the dictates of phase equilibrium theory, the concept of a phase being used in the sense of J.W. Gibbs. However Grant and Dunell [1,2] have quantitatively shown that, for stearic acid, crystalline and liquid phases can coexist in equilibrium over a wide range of crystallinity at temperatures below the melting temperature. Similarly, in experiments involving carefully controlled crystallization conditions for undiluted polymers, the coexistence of two phases in equilibrium at high levels of crystallinity is common. However, in polymers, amorphous regions, which are at various stages in the liquefaction process, are present throughout the lattice, whereas the liquid like regions in the stearic acid appear to have distinct boundaries, are characterized by rapid molecular diffusion, and, unlike polymers, do not pass through progressive stages in the melting process over a wide range of temperature. An equilibrium description would not be expected to characterize a substance composed of solid and liquid phases at temperatures other than the fusion point. Deviations from equilibrium at finite levels of crystallinity may be a common occurrence, and methods to describe such deviations quantitatively need to be developed. In addition, the existence of a crystalline phase does not imply that it is a perfectly constituted entity. Incorporation of lattice defects and imperfections of various kinds in the fatty acids and polymer systems are to be expected, in analogy with "regular" crystalline

Fig. 1a STEARIC ACID

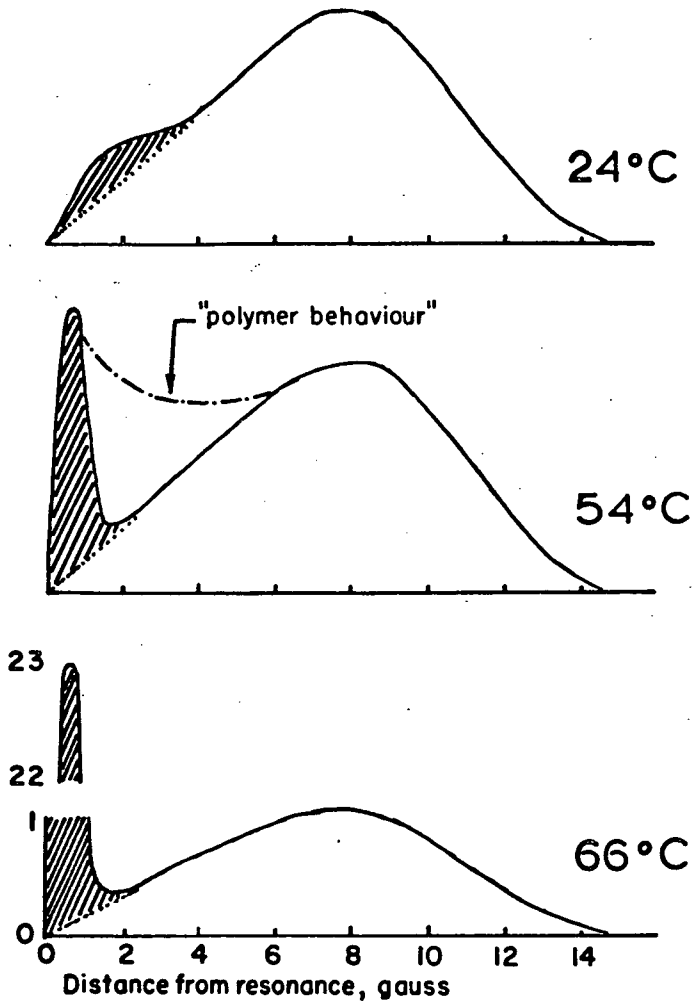

Fig. 1b POLYETHYLENE

C.W. WILSON III and G.E. PAKE
J. CHEM. PHYS.
27, 115 (1957)

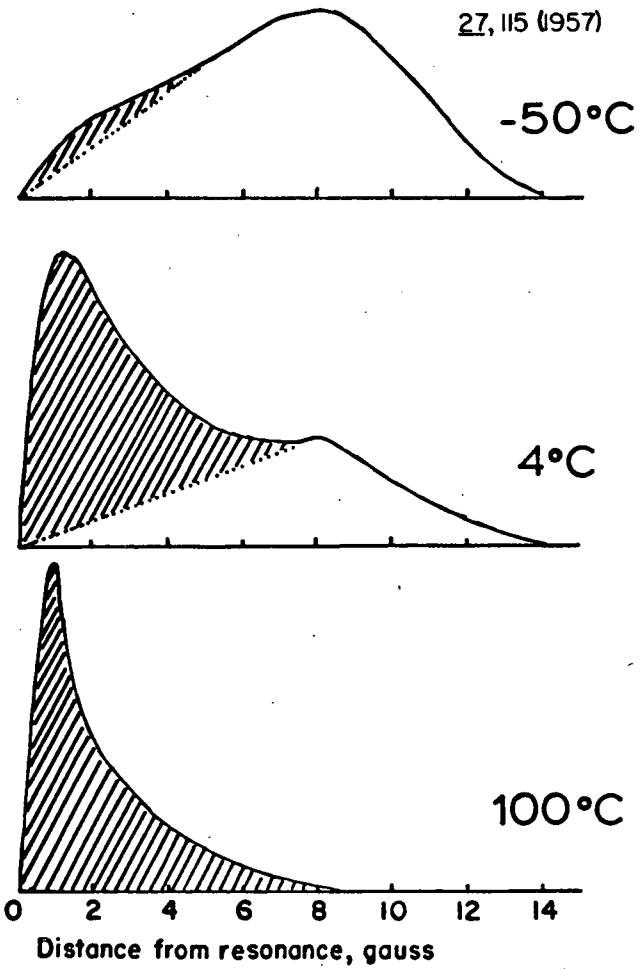

Examples of one half of first derivative curves of stearic acid (1a) and polyethylene, with decomposition lines, showing growth of narrow component (shaded region).

substances. Detailed description of such defects, particularly those which are predominant in paraffin systems, needs to be developed.

MOTIVATION

In 1960, Grant and Dunell[1,2] measured the broadline nuclear magnetic resonance (NMR) absorption of the C-form of stearic acid over the temperature range -78° to the melting point, 69.6°C. Their results suggest that very little molecular motion, other than small oscillations of the molecule and free rotation of the end-methyl group under the influence of temperature, occurs, except for premelting in isolated regions of the lattice, as the fusion temperature is approached. The "liquid-like" phase, which appears at temperatures above 20°C, exhibits itself as a narrow component on the broadline NMR spectrum (Fig.1a). Unlike the NMR absorption spectra of polymers, where the line-width of the amorphous component gradually decreases from an almost rigid lattice value of ca.15 gauss to the liquid-like value of ca. 10^{-3} gauss as the temperature is increased (Fig.1b), the narrow component line-width for stearic acid is less than 0.1 gauss.regardless of temperature, the change with temperature being in the amplitude of the narrow line. The observed line-width of between 0.1 and 0.01 gauss does not correspond to a liquid condition, for which a line-width of 10^{-4} gauss would be expected; nevertheless rapid molecular motion about several axes must certainly be occurring. The increasing amplitude of the narrow component suggests that more and more molecules begin to move rapidly as the temperature rises. Since the percentage area under the narrow component corresponds approximately to the percentage of the hydrogen nuclei that are in rapid motion, a plot of the integrated areas under the broad and narrow components of the proton resonance lines versus temperature is shown from the results of Grant and Dunell[1,2](Fig.2). As it is unlikely

FIGURE 2

FRACTION OF PROTONS
INVOLVED IN RAPID MOTION[1,2]

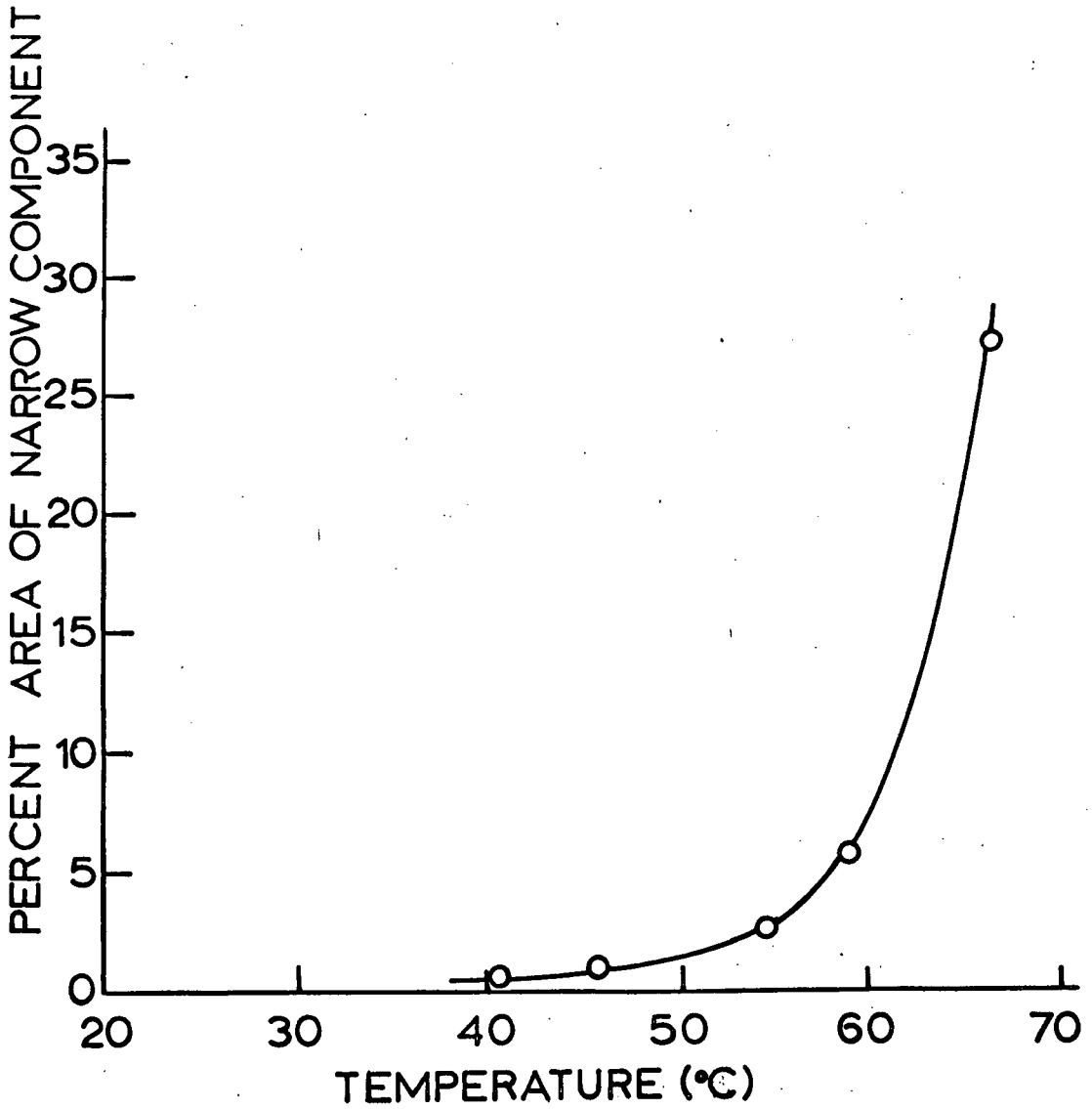

that portions of the individual stearic acid molecules are undergoing rapid reorientations about more than one axis[2,3], they suggest that the solid stearic acid is present in two phases. They suggest that the increase in the amount of liquid-like or disordered phase as the fusion temperature is approached may account for the anomalous expansion of stearic acid between 60° and 69°C as reported by Singleton, Ward and Dollear[4].

The purpose of this thesis is to enquire about the origin of this narrow component and to further investigage molecular motion in stearic acid.

BACKGROUND MATERIAL ON STEARIC ACID.

The special feature of the fatty acid structure is its stratification. In each stratum the molecules are arranged side by side and, if the acid is monobasic in character, the thickness of a stratum is approximately equal to twice the length of the molecule. In stearic acid each stratum consists of a layer of hydrogen bonded carboxylic functional groups. Away from this layer, in both directions, extend the paraffin portions of the molecules, as is shown in Fig.3. If a number of the strata were put together like the pages of this thesis, one could envision the end-methyl groups on the face of one stratum adjusting themselves so that they are fitted in some characteristic pattern with the end-methyls of the adjacent stratum. Each stearic acid molecule is held quite rigidly in its stratum as a result of the strong hydrogen bonding in the acid layer and of the van der Waals interactions, which are strong owing to the close packing of the adjacent hydrocarbon chains. Stearic acid has been observed in the A-, B-, and the C- crystalline forms[5,6]. Slightly below the melting point the C-form is the most stable, and in that region the other forms are irreversibly converted into the C-form. The transition

UNIT CELL OF STEARIC ACID

T. Malkin, "Progress in the chemistry of fats and their lipids," Pergamon Press, London, Vol. I, page I (1952)

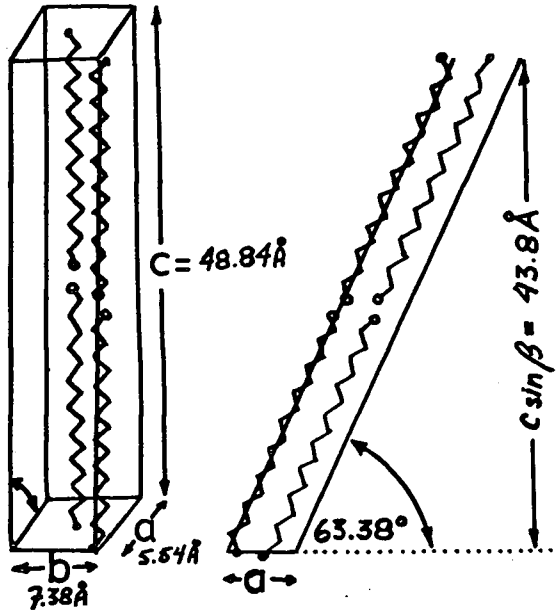

FIGURE 3

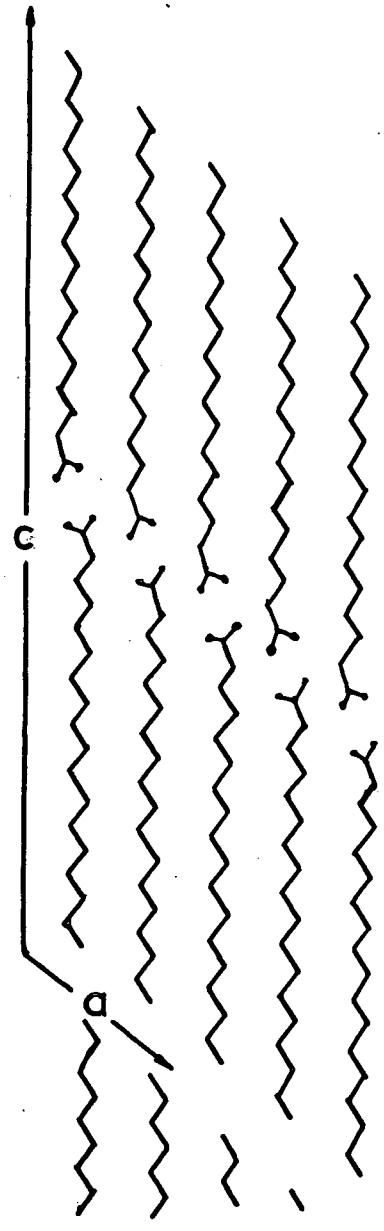

from the B- to the C-form of stearic acid is quite rapid at 53°C. Singleton et al[4] report that the transition to the C-form from the B-form occurs in 380 hours at 35.2°C. They also report that crystallization at temperatures above 53°C results in the stable C-form of stearic acid and at temperatures below 53° in the unstable B-form, regardless of the solvent used[4]. However, it is not quite clear what particular form is stable at the low temperatures. It is possible that at low temperatures, a transition from the C-form to the B-form or the A-form might occur if sufficient time were allowed. Von Sydow[3] reports that the A-form is obtained from acetone at low temperatures and that a mixture of the A- and C-forms is obtained from acetone at room temperature.

Dilatometric studies of stearic acid[4,7] show an anomalous increase in the volume of the acid at temperatures near the melting point as shown in figures 4a and 4b. From the broad sigmoidal nature of the dilation curve as compared to the sudden or sharp discontinuity which one would expect for a first order transition at the fusion temperature, one would suppose that a process other than a normal thermal expansion of the crystal is occurring. It is unfortunate that water has been used as the confining fluid in the dilation measurements shown in figure 4a[7], as it is quite possible that the anomaly could be a result of the penetration of water molecules into the acid structure. Singleton et al[4] do not state what confining fluid was used in their dilation measurements. There is no obvious explanation for the contraction of the stearic acid at temperatures greater than 20°. One important observation made during the dilatometric studies was the dependence of the physical characteristics on thermal history.

Fig. 4a Comercial stearic acid (impure)[14]

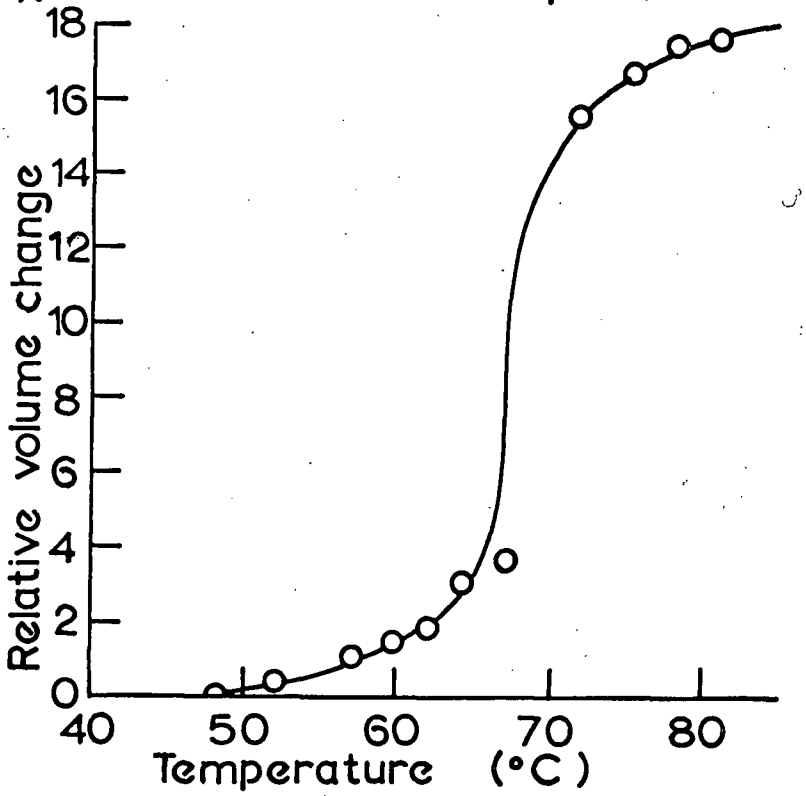

Fig. 4b

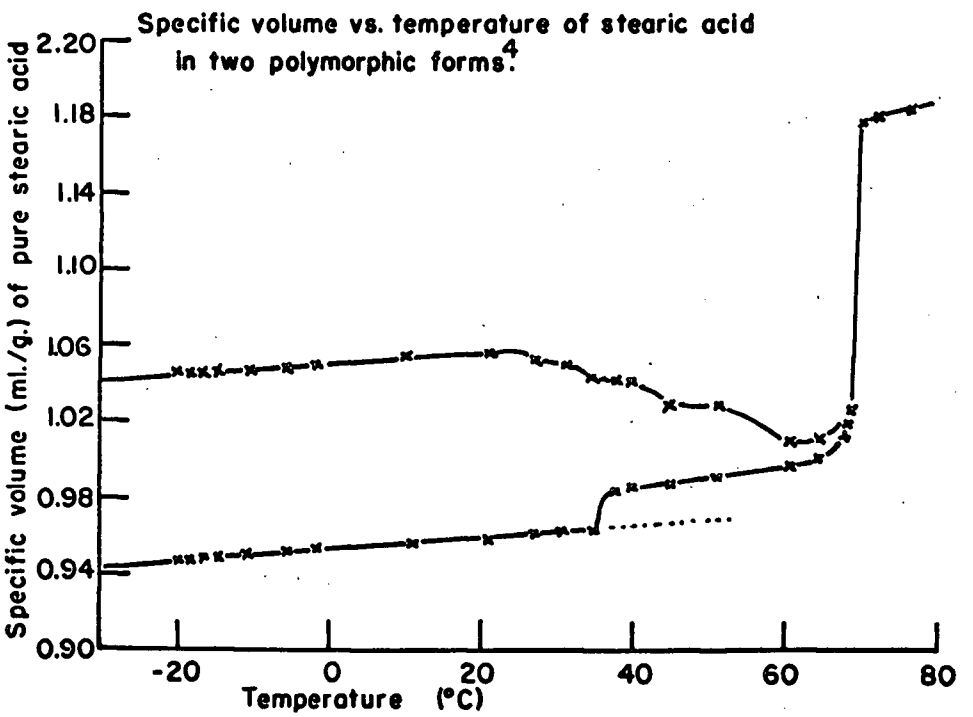

The results of Barr, Dunell, and Grant[8] in their measurements of NMR spectra andthe infrared absorption between 700 and 750 cm^{-1} serve to confirm this dependence on thermal history as well as to indicate the breakdown of crystalline character and the onset of liquid-like motion at scattered points in the solid structure several degrees below the fusion temperature. They note that the extent of liquid-like motion increases as the melting temperature is approached. In their analysis of the infrared absorption at 730 cm^{-1}, they attribute the observed doublet to a perturbation of the CH_2 rocking vibration by the interaction of nearest neighbour methylene chains in the crystalline array. They observe that the doublet gradually coalesces to a singlet as more and more molecules begin to move incoherently. Their infrared results give no indication as to the nature of the liquid-like phase or why two phases should coexist at all.

MOLECULAR MOTION IN STEARIC ACID.

Since the stearic acid dimers are very elongated and the crystal structure is lamellar, one should expect the formation of a smectic structure when the temperature is high enough to break the weak van der Waals bonds between the strata but when there is not sufficient energy to break up the sheets themselves. However, Gray[9], in discussing the structural requirements for mesomorphic behaviour, writes that the normal aliphatic fatty acids are not mesomorphic, irrespective of the length of the alkyl chain present in the molecule. He attributes this lack of mesomorphic character to the absence of a permanent dipole in the dimer and the normal paraffins, which fulfil the requirement of geometric anisotropy, but, yet, do not exhibit mesomorphic properties. However, Gray appears to have overlooked a report by Sidgwick[10], who writes that the fatty acid dimers do possess a small dipole moment.

Nevertheless it is probably true that any substance with anisotropic molecules would form a liquid crystal if it could be obtained in liquid form at a sufficiently low temperature, for if the molecules are asymmetric, or if the force fields around them are asymmetric, the internal energy of the liquid would be less if the molecules were all oriented parallel to one another, in an appropriate mutual relationship. In other words, a nematic form of the substance must have a lower energy than the normal amorphous liquid, and this in turn implies that the normal liquid will undergo transition to a nematic form if it is cooled sufficiently. Whether this nematic form can be observed in practice will depend on the melting point of the solid; in most cases the transition will be virtual since it will lie below the melting point[11]. Gray[12], and Brown and Shaw[13] agree that impurities can influence the formation of mesomorphic phases in certain nonmesomorphic compounds. Since the width of the narrow component on the NMR absorption line is larger than that which would be expected for liquid-like motion, 10^{-4} gauss, it is possible that the liquid-like regions of the lattice may be nematic regions, the formation of which is influenced by small amounts of impurity or by defect centres in the lattice.

Defect centres may be large amorphous regions (ca. 10^{3}A) or submicroscopic lattice disorders caused by stress, impurity molecules, or dislocations. Amorphous regions may be produced by cooling the melt rapidly; the internal friction increases so greatly that the molecules are unable to form a crystalline lattice. The amorphous state is that of a supercooled liquid; thermodynamically speaking it is unstable. The transition to the crystalline state, that is, annealing, may occur under suitable conditions and only very slowly (for example, consider crystallization in some ancient glasses). For the annealing process to occur, it is necessary

that the molecules be able to diffuse through the lattice, the rate at which molecules diffuse to the "correct" lattice sites being the rate of annealing. When the molecules are not in their lattice positions, but are in or adjacent to some defect centre, their packing may be disordered to the extent that the binding forces are somewhat weaker than those in the "perfect" lattice, allowing a greater degree of molecular motion compared to that in the perfect lattice. However, if the defect regions are indeed amorphous, that is, the stearic acid dimers are tangled and bent about in a manner characteristic of polymers, then one should expect a NMR absorption spectrum similar to those observed for polymers. Since the observed spectra do not resemble those of polymers, it is suggested that the defect centres are ordered in such a way as to give rise to a spectrum similar to that of the perfect lattice, at least until rapid diffusion begins.

Viscosity measurements on liquid stearic acid[14] (Fig.5) indicate that no transition from the liquid-crystal to the liquid stearic acid occurs above the fusion temperature. Crowe and Smyth[17], in their dielectric measurement studies of stearic acid, report that no rotation transition occurs in the solid stearic acid prior to fusion. This indicates that the fusion process of the stearic acid is mainly a sudden phase transition from a crystalline array to a liquid in which isotropic free rotation and diffusion occur very rapidly. If one could assume that the viscosity of the stearic acid in the liquid embryos lies on the extrapolated portion of the viscosity versus temperature curve (Fig.5), then the expected line-width of the liquid-like regions would certainly be less than 0.1 gauss[18,19,20]. High resolution NMR studies of the narrow component of the absorption signal might indicate whether the liquid embryos are nematic, liquid crystalline regions, or liquid regions.

FIG. 5

GRAPH OF
VISCOSITY VERSUS TEMPERATURE
OF PURE STEARIC ACID[7]

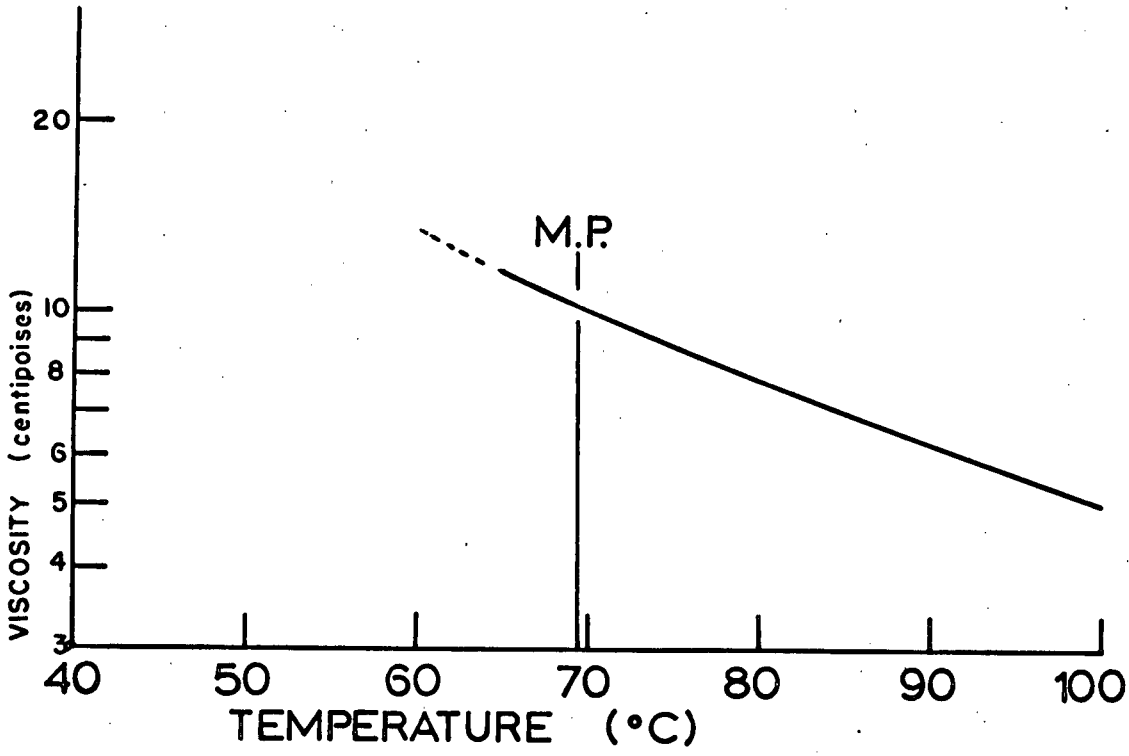

It would be interesting to speculate about the size of the liquid embryos that give rise to the premelting phenomenon as observed by Grant[1]. The observation that no "filling in" of the absorption curve (Fig. 1a and 1b) occurs as the transition temperature is approached implies that we have the following arrangement in the crystal: the liquid embryos are sufficiently large so that the molecules on the surface of the embryo compose less than 5% of the total member of molecules in the sample. The NMR spectrum of these "transition" molecules should fill in the spectrum as shown by the dot-dash line in figure 1a. However, since no filling in is observed, one may conclude that the effect of these transition molecules is less than the experimental error, say 5%, in the measurement of the integrated intensity of the signal.

If we assume these liquid embryos to be spherical in shape, with radius r, and volume $V = \pi 4r^3/3$, and that the transition region extends 10 A beyond the liquid zone, then if 10% of the molecules are undergoing liquid like motion we have:

$$dV = 4\, r^2 dr \pi$$

$$\frac{dV}{V} = \frac{0.05}{0.10} = \frac{3dr}{r}$$

but dr = 10 A, therefore

$$r = 60 \text{ A}$$

$$V = 904 \times 10^3 \text{ A}^3.$$

At 50° the specific volume of stearic acid[4] is 1.06 ml/gm or 1000 A^3 per dimer. Since the minimum volume of the "average" liquid embryo is ca. 900×10^3 A^3, then we should have approximately 900 dimers per liquid embryo. This somewhat oversimplified approach indicates that these liquid embryos must be large. It is almost certain that all liquid embryos are not the same size. Also, non-spherical embryos exist and cause the lower limit

in the number of molecules per liquid embryo to be increased in magnitude to accommodate the increased surface area of the embryo. Since the formation of these embryos is dependent on the heat of fusion and the solid liquid surface tension it seems probable that impurities, which severely affect the latter, should play an important role in the premelting phenomenon.

From the above discussion, it is clear that if one were to introduce various types of defects into the lattice one should be able to gain some insight into the type of motion occurring at these defects. A comparison between the NMR spectra of samples that have been quenched in ice or liquid N_2 and samples which have been cooled slowly and then, perhaps, annealed at 68° should illustrate the importance of physical defects. Similarly, samples with controlled amounts of impurity should illustrate the relative disruptive effect produced in the lattice by different impurity molecules.

THE EFFECT OF MOLECULAR MOTION ON THE NMR ABSORPTION SIGNAL

a) Theory

The width of the nuclear magnetic resonance absorption signal in most crystalline solids is due mainly to that part of the dipole interaction which conserves Zeeman energy. This conservation of Zeeman energy property has been utilized by van Vleck[21], who derived an expression for the second moment (or mean square width about the resonance centre) of the NMR signal in diamagnetic crystals. The expression he derives is valid for the rigid lattice, and for a polycrystalline substance in which the only magnetic species is the proton, the expression becomes

$$\text{Second Moment} = 716\ N^{-1} \sum_{i>j}^{N} r_{ij}^{-6} \qquad (1)$$

where N is the number of spins considered in the unit cell, and r_{ij} is the inter proton distance in Angstroms between protons i and j. The expression (1) involves the summation of

$$\left(\frac{3\cos^2\theta_{ij} - 1}{r_{ij}^3} \right) \qquad (2)$$

where the expression containing θ_{ij}, the angle the internuclear vector r_{ij} makes with the external magnetic field, H_0, has been averaged over all directions.

Subsequent treatments of the proton resonance signal for internal molecular motion are simple manipulations of (2). For example, Andrew[22], Dmitrieva and Moskalev[23,24], and Gutowsky and Pake[25] have developed the relations shown in (3) and (4) where ρ is a factor which reduces the r_{ij}^{-6} term in (1) by an appropriate amount for torsional oscillation through angle α of the interproton vector r_{ij} at angle γ to the axis of rotational oscillation.

$$\rho = 1 - (3/4)\left\{(1-J^2_0(\alpha)) \sin^2 2\gamma + (1 - J^2_8(2\alpha))\sin^4\gamma\right\} \qquad (3)$$

For free rotation (3) becomes

$$\rho = \tfrac{1}{4}(3\cos^2\gamma - 1)^2 \qquad (4)$$

where ρ and γ have the same significance as in (3).

However, it has been shown that the second moment should indeed be independent of molecular motion[26]. If one considers the molecular motion to be described by a characteristic frequency, $(\tau)^{-1}$, where $(\tau)^{-1}$ is the probable number of times per second at which the resonating particles involved jump or change their magnetic environment, one could visualize motional sidebands appearing about the NMR signal as a result of the modulation of the magnetic environments of the spins. These motional sidebands will, as a result of their distance from the resonance centre, contribute substantially to the second moment. However, the intensity of these motional sidebands is small and comparable in magnitude to the instrumental noise and, therefore, measurements are usually limited to the more intense centreband signal. Equations (3) and (4) apply reasonably well to the centreband signal[26].

The width of the NMR signal may be described by a characteristic time, T_2, often called the transverse or spin-spin relaxation time, where T_2 is defined as[27];

$$T_2 = \pi\, g(\omega_0) \qquad (5)$$

where $\pi = 3.14159...$ and $g(\omega)$ is the normalized intensity of the absorption signal at the centre band or larmor frequency, ω_0. To a fairly good approximation, T_2 is inversely proportional to the line-width at one-half height of the resonance signal. According to the theory of Bloembergen, Purcell, and Pound[28] as modified and confirmed by Kubo amd Tomita[29], the NMR spin-spin relaxation time for a nuclear dipolar relaxation in a system of two identical

nuclei undergoing isotropic Brownian motion in a heat bath is given by the following expression:

$$\frac{1}{T_2} = \sigma^2 \left\{ \tau + \frac{\frac{5}{3}\tau}{1+(\omega\tau)^2} + \frac{\frac{2}{3}\tau}{1+(2\omega\tau)^2} \right\} \qquad (6)$$

where σ^2 is the Van Vleck rigid-lattice second moment and τ, the correlation time, is the time between fluctuations of the magnetic field of one nucleaus at the site of the other. However, for systems of more than two identical nuclei in which the motion of each nucleus may or may not be dependent on the motion of other nuclei, the expression becomes prohibitively difficult to determine. Usually one speaks of an average correlation time, τ, of a distribution of correlation times, the distribution being dependent on the substance considered and on its temperature. If the distribution of the correlation times is narrow, the expressions (6) and (7) are usually assumed to be correct.

When one describes the rate of exchange of nuclear spin energy with the host material or lattice, a characteristic time, the spin-lattice relaxation time, T_1, is used. In a diamagnetic solid, where dipole interactions only are considered, the most obvious mechanism to couple the nuclear spins to the lattice is the fluctuation of the local magnetic fields which arises from the lattice vibrations simply because the strength of the field at one nucleus due to the dipole moment of a neighbour depends on the distance between them. In the case of two identical nuclei undergoing isotropic Brownian motion, the expression relating T_1 to the correlation time is [29]:

$$\frac{1}{T_1} = \sigma^2 \left[\frac{\tau}{1+(\omega\tau)^2} + \frac{4\tau}{1+(2\omega\tau)^2} \right] \qquad (7)$$

where σ^2 and τ have the same significance as above. However, in practice, the T_1 observed is usually very much less than that predicted by theory. The difference between the two is usually attributed to the presence of paramagnetic impurities in the sample.

b) The experiment.

For liquid-like diffusion, the second moment of the resonance absorption is reduced to several milligauss^2, small compared to the usual values of 3 to 30 gauss^2 for diamagnetic solids or even to the value of approximately one gauss^2 observed for isotropic free rotation but without translation of the molecules in their crystal lattice. Similarly, the line-width of the NMR signal ranges from several milligauss, for liquid-like motion, to as high as 20 gauss for the rigid lattice signal.

Liquid regions in the solid lattice will give rise to a narrow sharp signal superposed on the broad absroption signal of the more rigid lattice (Fig.6). The integrated intensity of the two components will allow the experimenter to determine the relative number of protons undergoing liquid-like motion (isotropic free rotation and diffusion where $(\tau)^{-1}$ is very much greater than the line-width as expressed in frequency units), compared to those whose motion is slow compared to the line-width (as expressed in frequency units).

The most satisfactory method of estimating τ, an average correlation time for the bath, is through measurement of the spin-lattice or thermal relaxation time, T_1. Very approximate values for τ may be also obtained from line-width and second moment measurements[30,31] but such evaluations require that the molecules be simple and that the motion be uncomplicated if valid results are to be expected. Evaluations of τ, using T_1 measurements,

complement the information obtained from line-width and second moment measurements and extend measurements beyond the melting point.

When the motions of the resonating nuclei can be characterized by a single correlation time, the NMR relaxation time, T_1 may be calculated from the expression (7). τ is assumed to have the form:

$$\tau = \tau_\infty \exp(\Delta E/RT) \qquad (8)$$

where ΔE is the activation energy of the relaxation process and τ_∞ is a constant of the system having dimensions of time. This Arrhenius relation, (8), may be too simple to describe τ as ΔE may itself be a function of temperature. If T_1 is plotted versus $1/T$, the curve passes through a minimum when $\omega_0\tau = 0.61579.....$ This equality is obtained by equating the first derivative of (7), with respect to τ, to zero. Usually T_1 minima occur when molecular motions take place at frequencies of the order of 10^8 sec^{-1}, since the larmor frequency is typically of the order of 10^7 to 10^8 sec^{-1}.

EXPERIMENTAL PROCEDURE

This section is devoted to a description of the experimental equipment used to obtain the data to be presented in succeeding sections, and to a brief explanation of the experimental procedure.

PROCEDURE OF MEASUREMENT AND ANALYSIS OF DATA.

The quantity measured in these experiments was the derivative of the NMR absorption signal. To obtain this, the r.f. transmitter was held at a constant frequency while the main magnetic field was varied by means of a scanning unit which utilized a Synchronous-motor driven potentiometer which in turn governed the chopper amplifier of the regulated power supply for the electromagnet (field H_0). Superposed on the main magnetic field, H_0, was a small modulated field $H_m = h_m \sin \omega_m t$. The receiver network was phase sensitive with respect to the modulation frequency ω_m. In all cases, in these experiments, h_m and ω_m were kept sufficiently small so as not to alter significantly the lineshape of the absorption signal.

a) Premelting:

The liquid-like regions signal had a width of several milli-gauss, whereas the width of the line for the more rigid lattice was about 14 gauss. Thus the absorption due to the protons in the non-liquid constituents was essentially constant over the narrow frequency region occupied by the liquid signal, and accordingly the intensity of the latter was used for a quantitative measure of liquid content. Experimentally, one obtains a derivative of the absorption curve and it was convenient to measure the relative peak to peak amplitudes of the two components (Fig. 6). The procedure was standardized by constructing a calibration curve by plotting the relative integrated

intensities of the two components versus the relative peak to peak amplitudes (Fig. 6).

The relative integrated intensity was obtained for the wide component of the derivative signal by applying the following relation to each half of the derivative curve (see Appendix A):

$$\text{Area} = \delta^2 \sum_{n=1}^{\infty} g(n) \qquad (9)$$

where g(n) is the signal amplitude at n increments, each of magnitude δ gauss, from the centre of resonance. The area or integrated intensity for the broad component is then the sum of the areas for each half of the spectrum. The summation was made sufficiently accurate by limiting the magnitude of the increments (δ). It was found, however, that fairly large increments (about 1/15-th the line breadth) could be used without significantly affecting the area. For the narrow component, the relative integrated intensity was obtained from the product of 1/3 the peak to peak amplitude and the modulation amplitude squared, h_m^2 (see Appendix A). The U.B.C. computer was utilized for the calculations. (see Appendix B for a description of the computer programs).

In practice, the sharpness of the narrow component necessitated care in maintaining the same receiver response and scanning rate for all spectra. The reason for this is illustrated by considering a detecting system with response time, T*, responding to a signal, S_0, when the time spent on the signal is t. The response of the detecting system is then described by the relation:

$$S = S_0(1 - \exp(-t/T^*)) \qquad (10)$$

where S is the output from the detector system. In practice, the modulation of the main magnetic field by $H_m = h_m \sin \omega_m t$ effectively smears out the liquid signal to a width comparable to h_m, the modulation amplitude. Thus,

FIG. 6

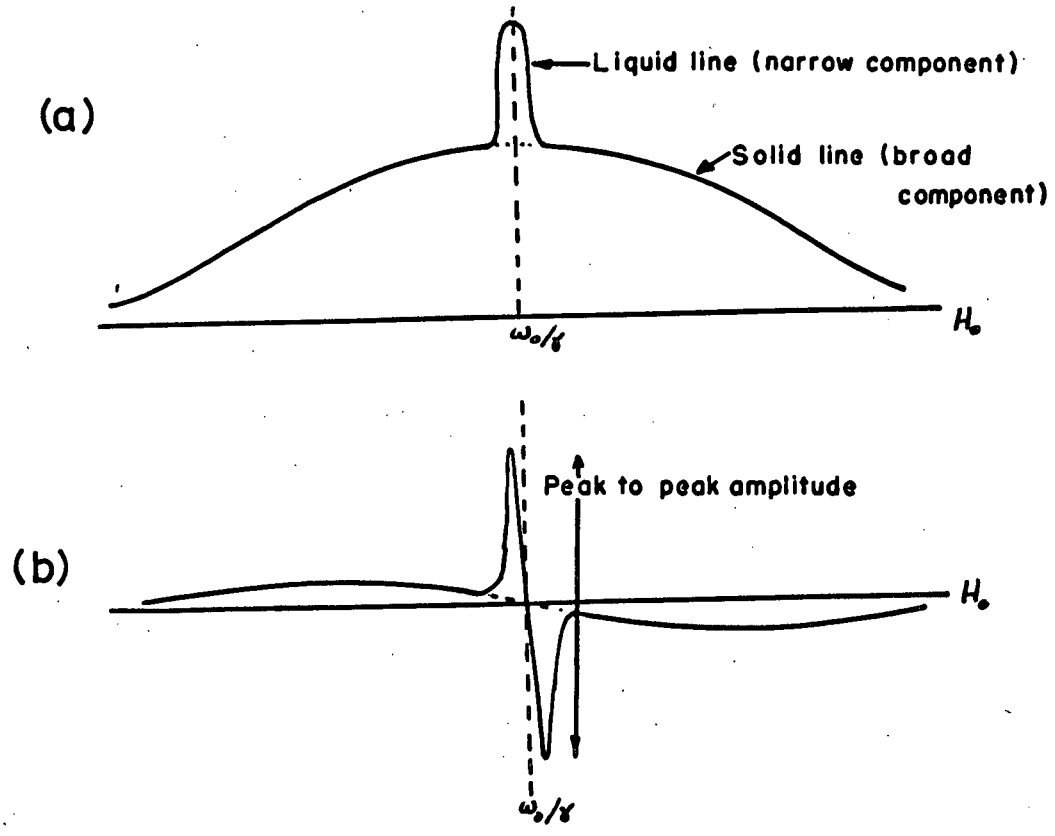

Proton resonance signal (schematic) of liquid regions in solid material. (a) Absorption signal (b) Derivative signal

since the scan rate is very slow, t is large and S is approximately equal to S_0.

Other sources of error could arise from the nonlinearity of the detector system. However, frequent instrument checks usually limit this error or uncertainty to less than one per cent.

b) SPIN-LATTICE RELAXATION TIME, T_1, MEASUREMENTS

The spin-lattice relaxation times, T_1, were determined by means of the following methods; the adiabatic rapid passage experiment as described by Drain[32] and Chiarotti[33], the signal recovery technique described by Linder [34] and by means of the progressive saturation method described by Bloembergen, Purcell, and Pound[28]. The effect of the spin-lattice interaction is to relax the spins to their equilibrium state in a time T_1. In solids, the spins interact strongly with one another so that energy absorbed at one frequency of the dipolar broadened resonance line is quickly transferred to all spins, whether or not they are all in a local field exactly corresponding to the applied r.f. frequency, in a time T_2. According to Bloembergen et al[28], the complex r.f. susceptibility is proportional to the difference in population of the nuclear spin levels and is only affected by the presence of the r.f. field in so far as the spin level populations are. Using these criteria, complete saturation should occur when the spin level populations are equal. The recovery from saturation technique of Linder involves allowing the spin-system (i.e. sample) to come to equilibrium with a strong r.f. field, turning off this field, and with a very weak (very much less than that required for saturation) r.f. field, watching the signal recover from saturation. If S is the signal amplitude, then the equation for signal recovery is:

$$S = S_0(1 - \exp(-t/T_1)) \qquad (11)$$

FIG. 7

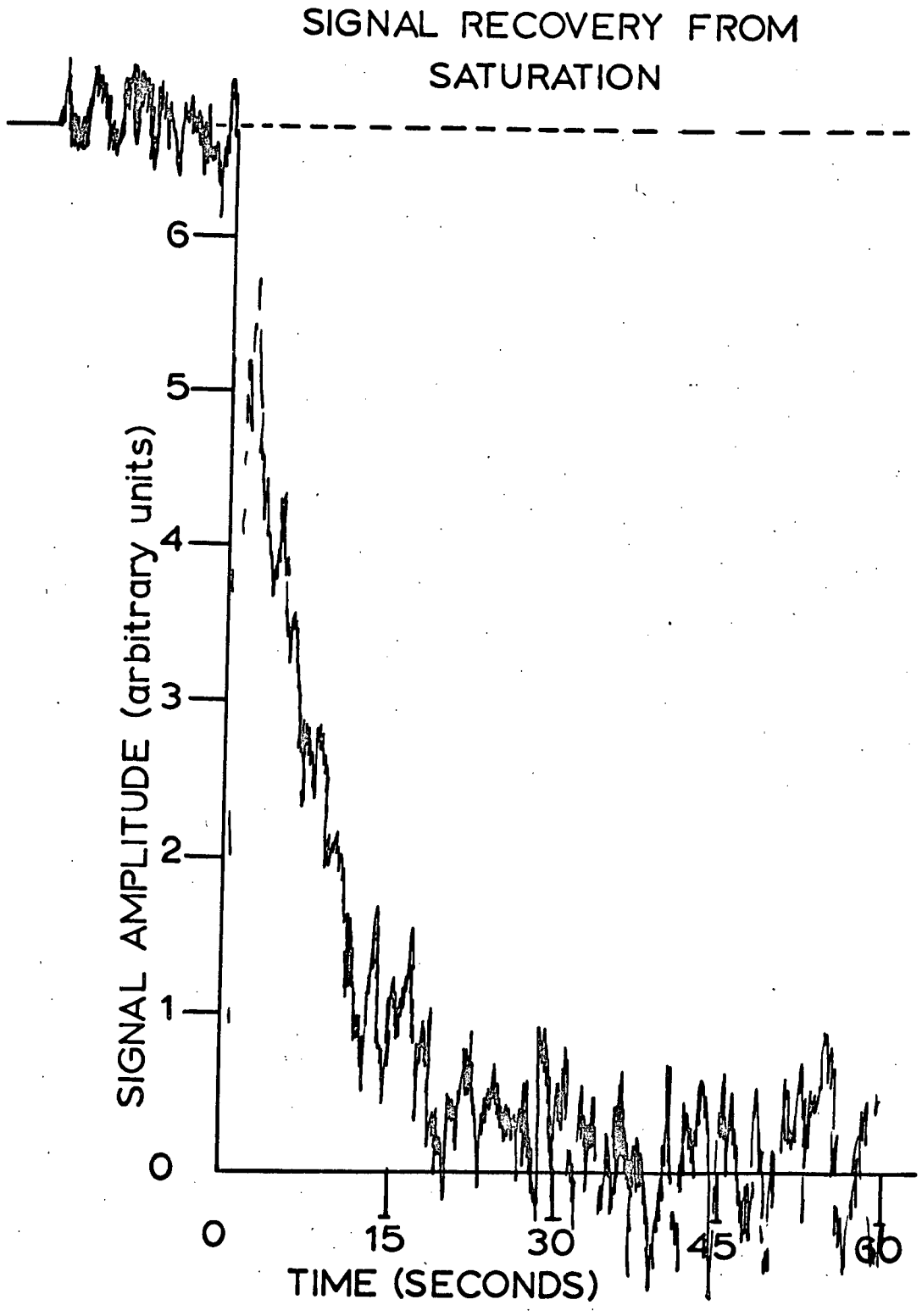
SIGNAL RECOVERY FROM SATURATION
SIGNAL AMPLITUDE (arbitrary units)
0
1
2
3
4
5
6
0
15
30
45
60
TIME (SECONDS)

A typical recovery curve is shown in Fig. 7. The signal in this case was the derivative maximum (assumed to be directly proportional to the intensity of the actual absorption signal at any frequency) of the absorption signal. T_1 is obtained directly from the slope of a semi-logarithmic plot of (11). Unfortunately the time constant T* of the detecting system, about 1 second, limited measurement of T_1 to T_1 greater than 3 seconds. The sensitivity of the receiver was low and required a fairly high r.f. field to observe the recovery and thus T_1 measurement was limited to T_1 less than about 10 seconds. The T_1 values obtained by this method should be slightly longer than the actual T_1 of the system since the observing r.f. field intensity "slows down" the recovery.

The progressive saturation technique involves plotting the absorption signal amplitude versus r.f. field intensity. According to Bloembergen, Purcell, and Pound[28] the signal amplitude reaches a maximum when the saturation factor $\gamma^2 H_1^2 T_1 T_2 = 1$. In practice, the r.f. field meter reading, μ_m, of the 16 Mc variable frequency transmitter was directly proportional to H_1. This was verified by W. Janzen who used a method described by Anderson to measure the H_1. Generally, one assumes that T_2 is inversely proportional to the line-width as long as the line shape remains constant. Therefore one can write the saturation factor for this condition as:

$$\frac{T_1 \mu_m^2}{\delta H} = \text{constant.} \qquad (12)$$

Then, knowing a T_1 value at a particular temperature, one should be able to determine the constant in (12) and determine T_1 values at other temperatures where the line-width has been predetermined.

Bloembergen has pointed out that the Bloembergen, Purcell, and

Pound[28] (B.P.P.) theory must be incorrect when a large r.f. field is applied to a solid, in which $T_1 \neq T_2$, because in the limit as $H_1 \rightarrow \infty$ the B.P.P. theory predicts the line-width to be $\gamma H_1 \sqrt{T_1/T_2}$ rather than γH_1 as required by the uncertainly principle[35] and the transition probability associated with the r.f. field.

Redfield[36] and Goldman[37] show that at high r.f. fields the behaviour of the absorption signal is very complicated and that behaviour is further complicated by the field modulations associated with detecting the derivative signal. Furthermore, incorrect phasing of the lock-in detector with the modulation frequency introduces errors where the measured T_1 differs from the true T_1 by a factor of two or three although saturation would still occur according to (12) but with the constant different from that which one would expect if B.P.P. theory were applied. Goldman[37] shows that the ratio of the modulation frequency to the line-width and T_1 is important in the saturation factor, but the expressions showing these relations are too complicated to be presented here.

The adiabatic fast passage technique described by Drain [38] involves modulation the magnetic field at amplitudes of ca 100 gauss and at frequencies of the order of $1/T_1$ so that the following modified conditions will be satisfied:

$$\frac{\delta H}{T_1} \ll \frac{dH_0}{dt} < \gamma H_1 \delta H \qquad (13)$$

According to Chiarotti [39], the in phase component (dispersion) of the r.f. susceptibility should, under the above rapid passage conditions, follow the behaviour:

$$M = M_0 \left| \frac{(1 - \exp(-\tau/T_1))}{(1 + \exp(-\tau/T_1))} \right| \qquad (14)$$

where M is the magnetization in the z-direction (collinear with H_0), M_0 is the equilibrium magnetization in the absence of an r.f. field, and τ is the

FIG. 8

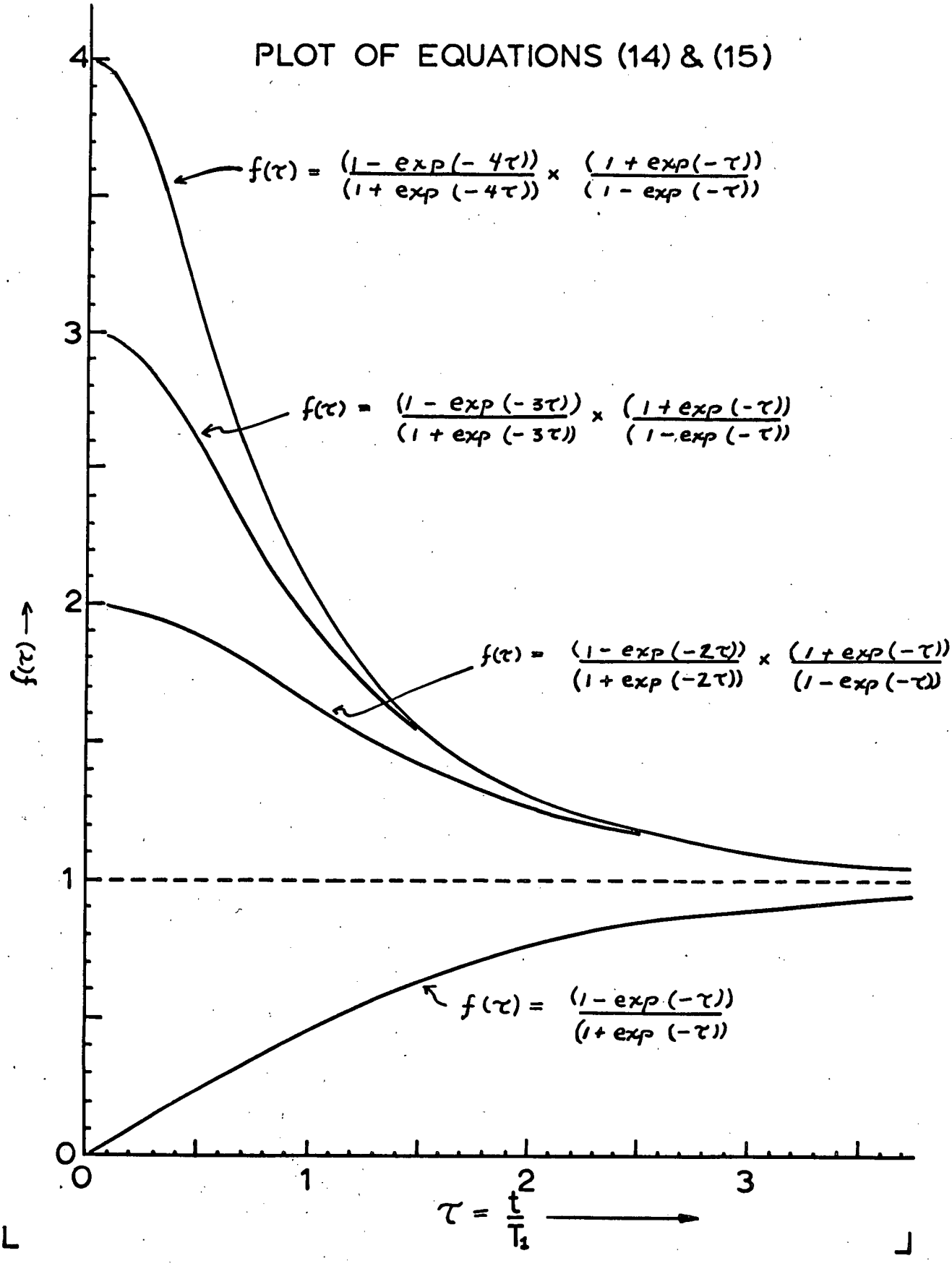
PLOT OF EQUATIONS (14) & (15)
$f(\tau) = \frac{(1-\exp(-4\tau))}{(1+\exp(-4\tau))} \times \frac{(1+\exp(-\tau))}{(1-\exp(-\tau))}$
$f(\tau) = \frac{(1-\exp(-3\tau))}{(1+\exp(-3\tau))} \times \frac{(1+\exp(-\tau))}{(1-\exp(-\tau))}$
$f(\tau) = \frac{(1-\exp(-2\tau))}{(1+\exp(-2\tau))} \times \frac{(1+\exp(-\tau))}{(1-\exp(-\tau))}$
$f(\tau) = \frac{(1-\exp(-\tau))}{(1+\exp(-\tau))}$
$f(\tau) \rightarrow$
$\tau = \frac{t}{T_1} \rightarrow$
0
1
2
3
4

time between passages through resonance. If the modulation frequency is Ω, then $\tau = (2\Omega)^{-1}$. A square wave modulation of H_0 is used so that passage through resonance will be rapid but the extrema in H_0 will be sufficiently close to resonance that the magnetization (proportional to H_0) will relax to essentially the same value of M_0. In practice the sweep range of ca 100 gauss is small compared to H_0, ca 2.62 kgauss. The time spent on resonance, i.e., the time required to sweep through the signal, was 0.018 seconds. This time is short compared to T_1. The r.f. field, H_1, was approximately 0.2 gauss and thus $\gamma H_1 \delta H$ was approximately 10^5 gauss/sec, large compared to $dH_0/dt \approx 10^3$ gauss/sec, and $\delta H/T_1 < 1500$ gauss/sec. since $\delta H \approx 15$ gauss and $T_1 \geq 10^{-1}$ sec. Since M_0 is unknown and only relative values of M are known, (14) the value for T_1 was determined by considering the ratio of M to M' for sweep periods τ and τ' thus:

$$\frac{M}{M'} = \frac{\left(\frac{1-\exp(-\tau/T_1)}{1+\exp(-\tau/T_1)}\right)}{\left(\frac{1-\exp(-\tau'/T_1)}{1+\exp(-\tau'/T_1)}\right)} \qquad (15)$$

Normally $\tau = 2\tau'$, $3\tau'$ or $4\tau'$ in the experiment. A plot of M/M' versus (τ'/T_1) for values of (τ'/T_1) ranging from zero to 4 is shown in Fig. 8. A plot of M (eq. 14) versus (τ'/T_1) is also shown in Fig. 8. It is obvious from Fig. 8 that the greatest accuracy in determining τ'/T_1 from the ratio M/M' is obtained when τ'/T_1 and τ/T_1 differ only slightly from 1.

APPARATUS

Broadline NMR spectra were obtained with a Varian model V-4200 spectrometer with a fixed 56.4 Mc. frequency unit V-4311 and a Varian 12-inch pole face diameter electromagnet with regulated power supply model V-2100. The output was displayed by a Speedomax-G rectilinear recorder adjusted so that it had a response time of less than one second. The output signal trace was the derivative of the absorption curve.

Recovery from saturation and progressive saturation T_1 measurements were obtained with a Varian model V-4200 spectrometer with a variable frequency unit V-16 and a Varian 6-inch pole face diameter electromagnet with a regulated power supply. Measurements were recorded at 16 Mc. The output was displayed on a Speedomax-G rectilinear recorder adjusted to a response time of less than one second. The output signal trace was the derivative of the absorption curve. The r.f. field meter of the V-16 unit was calibrated by W.R. Janzen who used a technique described by Anderson[41].

Adiabatic rapid passage measurements were obtained with the above 16 Mc unit at maximum r.f. output ($H_1 \sim 0.2$ gauss). The in-phase component of the magnetization was rectified and displayed on a Dumont type 304 cathode-ray oscilloscope with external capacitors to lengthen the time base to about 30 seconds and the display was synchronized externally with the square wave generator, Hewlett Packard model 202A, which modulated the sweep input of the magnet power supply. The model V-2100 power supply responded slowly to the square wave signal, the response being governed by the high inductance of the 6-inch electromagnet. The sweep frequency was thus limited to less than 12 cycles per second. The sweep amplitude was normally set at approximately 120 to 200 gauss.

The samples were placed in 6 mm. O. D. Pyrex thin-walled sample tubes. These were maintained at the higher temperatures by arranging the sample container in a dewared assembly (which fitted within the Varian NMR probe) through which hot air passed from an external heater. Thermal inertia was provided the system by careful insulation of the entire assembly and by using a coil composed of 15 meters of $\frac{1}{4}$ inch copper tubing immersed in a 10 liter constant temperature water bath. By means of this assembly, temperature regulation to better than plus or minus 0.1°C was achieved over a

three day period.

All measurements at 77°K were obtained by immersing the sample directly in liquid nitrogen while recording the spectra.

The low temperature T_1 measurements were obtained with one sample of very pure stearic acid in a 10 mm. O. D. thin walled pyrex sample tube. Temperature regulation was obtained by passing cold dry nitrogen gas over the sample which was placed in a specially constructed dewar. The number of low temperature measurements was limited as the apparatus consumed a tremendous quanity of nitrogen for each measurement.

PREPARATION OF SAMPLES

The stearic acid used in this investigation was Eastman Kodak white label grade with freezing point of 66.5°C. The stearic acid was purified by fractional distillation then by numerous crystallizations at -20°C from freshly distilled reagent grade acetone, after the method outlined by Brown and Kolb[42]. The stearic acid was then "cured" under vacuum for eight days at 68° to 69°C. The reason for this curing process was to remove any solvents present and to be certain that the stearic acid obtained was the C-form. Markley[7] suggests that crystallization from solvents may yield a mixture of the B- and C-forms. However, the unstable A- and B-forms are irreversibly converted at temperatures about 15°C below the melting point, 69.4°C, into the stable modification, the C-form. A portion of this stearic acid was melted and the freezing point, 69.3°C, was obtained from the plateau of a time-temperature cooling curve run on a 5 gram sample using a calibrated thermometer. This value agrees well with the best setting points obtained by Francis[43], viz. 69.35° and 69.32°C. Francis found that 1% palmitic acid impurity added to stearic acid lowered the setting

point to 69.08°C. from 69.32°C.

Samples were prepared by adding small weighed quantities of purified impurities to weighed amounts of stearic acid (approximately 0.3 gram samples). The palmitic acid used as an impurity was Eastman Kodak white label grade and was purified in the same fashion as described above. The oleic and elaidic acid were purchased from the Hormel Institute[44] and were estimated to be better than 99% pure. The water was distilled, outgassed, and then added to the outgassed stearic acid in the vapour state. In all cases these samples were fused so as to distribute the impurity homogeneously throughout the sample and then annealed eight to ten days at temperatures near 69°C. The samples were all treated identically, all being cooled to room temperature at the same rate, and heated at the same rate when measurements were taken. In each case, the quantity of impurity added to the stearic acid was known to better than plus or minus 2% of the amount added.

The sample used for the T_1 measurements was a 7 gram quantity of pure stearic acid fused, outgassed and then sealed under vacuum. The sample was annealed for 14 days at 68°C and then cooled very slowly to room temperature.

EXPERIMENTAL RESULTS AND THEIR INTERPRETATION

Derivative spectra of the absorption signal of pure stearic acid were recorded at 77°K and at temperatures greater than 293°K. The experimental second moment decreases gradually from 28 gauss^2 at 77°K to 19.6 gauss^2 at 342°K (69°C). The line-width decreased gradually from 15.4 gauss at 77°K to 14.2 gauss at 342°K. The experimental second moment and line-width measurements confirmed those of Grant[1]. The problem is to account for the observed second moments in terms of equations (1), (3) and (4) and various molecular models.

The theoretically calculated second moment differed somewhat from that of Grant[1] in that the value 24.4 gauss^2, obtained by Grant[1], was 3.2 gauss^2 less than the value 27.6 gauss^2 calculated in this thesis. The intramolecular second moments 18.4 gauss^2 (Grant) and 19.8 gauss^2 (our value) were evaluated from the same model of the paraffin chain and acid group. The C-C and C-H bond distances were 1.54 Å and 1.09 Å, respectively, while all bond angles were assumed to be tetrahedral, 109°28'. The difference may arise from the fact that Grant limited interactions to a distance of 5 Å whereas all dipole interactions were considered in this calculation and Grant's assumption the C-H bond distances are 1.094 Å. The intermolecular second moment calculated by Grant was 6.0 gauss^2. This was evaluated from the known crystal structure of lauric acid at room temperature and the reasonable assumption was made that the intermolecular second moment should not be too different for stearic acid. It is quite probable that this value, 6.0 gauss^2, is too small for the rigid lattice conditions at low temperatures, say 77°K. A complete crystal structure study of stearic acid has not been published to date, and, hence, various approximations must be made.

The intermolecular second moment, 7.8 gauss^2, which Andrew[45] finds to be an appropriate value for long-chain n-paraffins at low temperatures, was used in the evaluation. The total second moment, SM_T,

$$SM_T = SM_{INTRA} + SM_{INTER}$$

$$= 19.8 \text{ gauss}^2 + 7.8 \text{ gauss}^2$$

$$= 27.6 \text{ gauss}^2$$

agrees very well with the experimental second moment, 28 gauss^2, for stearic acid at 77°K. For comparison with theory the experimental second moments are the mean of those obtained from about three sets of measurements. The probable error of the mean is about one gauss^2. No allowance is made for magnetic field inhomogeneity as the inhomogeneity was certainly less than 10^{-2} gauss.

Molecular motion typical of the solid crystal is limited to vibrational oscillations about a rotational axis and perhaps free rotation of the methyl group terminating the paraffin chain. The various types of motion about a rotational axis which may be encountered in the paraffin chain include[45]:

(1) rotation

(2) quantum mechanical tunneling through the potential barrier. The rotational axis should also be a symmetry axis if this motion is to be possible.

(3) rotational oscillation.

For a motion to be effective in reducing the line-width and second moment it should occur at a frequency greater than the half-width of the resonance line. Free rotation of the end methyl group on stearic acid should reduce the second moment for intramolecular interactions by 1.9 gauss^2. If the intermolecular SM is reduced by a proportionate amount, the total second moment should be 24.8 gauss^2. However, the crystal lattice expands under the

influence of temperature. If Grant's intermolecular SM value, 5.3 gauss^2, assuming CH_3 free rotation and room temperature crystal parameters, is added, one has a resultant SM of 23.2 gauss^2. At room temperature, it seems probable that much motion of the entire paraffin chain, in the form of rotational oscillation about the long axis and perhaps flailing of the end of the paraffin chain, should occur and reduce the second moment to 20 gauss^2 as is observed[1]. This picture agrees with the dielectric studies of Crowe and Smyth[46] who found no evidence of a rotational transition below the melting point of stearic acid.

It can easily be shown that for stearic acid the reduction in second moment due to the effect of zero-point energy oscillations of the protons in the paraffin chain is almost negligible. The correction factor for a single mode of motion is [47,48,49]

$$(1 - 3/2(\Theta)^2)^2$$

where Θ, the angular amplitude of oscillation, is given by

$$\Theta = \left(\frac{\hbar}{4\pi^2 c I \bar{\nu}}\right)^{\frac{1}{2}}$$

where c is the velocity of light, I is the moment of inertia of the oscillating group of atoms, and $\bar{\nu}$ is the frequency of oscillation in cm^{-1}. The methylene rocking mode, 725 cm^{-1}, is of a sufficiently low frequency to be of importance. The moment of inertia of the methylene group is of the order 4×10^{40} gm cm^2, if some interaction with the paraffin chain is also considered. The resulting reduction inthe second moment[1] is about 3 per cent or 0.8 gauss^2. Where I is larger, that is, more of the paraffin chain is considered, the resultant reduction in SM is less. The calculated SM for the rigid lattice with zero point vibrations should be 26.2 gauss^2 or 1.8 gauss^2 less than the experimental result. This value, 26.2 gauss^2, lies outside the expected experimental error and

perhaps may be accounted for by the model of the paraffin chain used or that the moment of inertia, used above, is too large. Dunell[2], Andrew[45], and Rushworth[50] are of the opinion that methyl group reorientation about the C_3 axis occurs at a significantly high frequency at 77°K to affect the second moment. Thus if CH_3 reorientation is occurring, the rigid lattice SM value should be 23.0 gauss^2, a value far below the observed 28 gauss^2 SM at 77°K. It is significant that Rushworth[50] calculates an intermolecular second moment of 9.6 $\pm$ 1.5 gauss^2 for n-pentane and n-hexane. If the intermolecular SM is increased from 7.8 gauss^2 (Andrew[45]) to 9.6 gauss^2 (Rushworth[50]) for solid stearic acid, then the rigid lattice SM is 29.4 gauss^2 and the SM for methyl reorientation plus zero point motion is approximately 24.8 gauss^2. Another model for the stearic acid molecule was chosen. The lauric acid structure is known[51]. The coordinates of the last six carbon atoms on the paraffin chain were shifted so that a six carbon insert could be made into the paraffin chain. The C-C and C-H bonds were 1.54 A and 1.09 A respectively. The bond angles of the six carbon insert were tetrahedral. The intramolecular second moment calculated from this model was 19.8 gauss^2, which is the same as that evaluated from Grant's more simple model. Muller[52] writes that the intramolecular dimensions of a crystalline normal paraffin should be relatively independent of temperature while intermolecular dimensions should be temperature dependent as a result of the comparatively weak intermolecular interactions. The intermolecular second moment may be significantly greater than 9.6 gauss^2 for the rigid lattice.

This discussion indicates that the significant motion at 77°K is certainly restricted to the end-methyl rotation and does not involve larger portions of the paraffin chain. The spin-lattice relaxation time results obtained in this thesis indicate that the rotation frequency of the methyl group at 77°K is 4×10^5 sec^{-1}.

PREMELTING IN STEARIC ACID

Typical broadline spectra for pure stearic acid, shown in Fig.9, are decomposed into a wide and narrow component for solid and liquid regions in the sample, respectively. The narrow component of the broadline spectrum is interpreted as being caused by large liquid regions in the solid lattice. The relative integrated intensities of the two components are interpreted as a measure of the liquid and crystalline regions, respectively, in the sample. The effect of added impurities and thermal history on the crystallinity of stearic acid is shown in Fig. 10 and 11.

In the introduction, it is shown that the number of molecules composing the solid-liquid interface must comprise only a few per cent of those molecules undergoing liquid-like motion as seen by NMR. The nature of the solid liquid interface is not understood well. It is important to note, however, that insofar as no intermediate phases are known for pure stearic acid, there should be only one interface bounded on both sides by solid and liquid respectively. The size of the liquid regions should be large enough so that the liquid regions, akin to a super-cooled liquid, will have a finite lifetime. If one applies a simple Boltzmann distribution to the kinetic energies of the molecules in the solid, it is conceivable that a certain number of molecules will have sufficient energy to diffuse rapidly or behave as a liquid. Consider the extreme example of a one molecule "liquid" region, that is, one molecule that has sufficient energy to diffuse repidly through the lattice. The lifetime of this one molecule liquid will be very short as it will lose its kinetic energy very rapidly to its neighbour molecules. Thus the concept of a minimum size in the liquid region is introduced in the sense that the surface area of the liquid region is important. Frenkel[54] interprets this in terms of the surface free energy of a liquid molecule on the boundary of the liquid-like region. Of course the heat of fusion of the sample is important here. It is discussed the introduction that the measure-

FIG. 9

TYPICAL BROADLINE SPECTRA FOR PURE STEARIC ACID

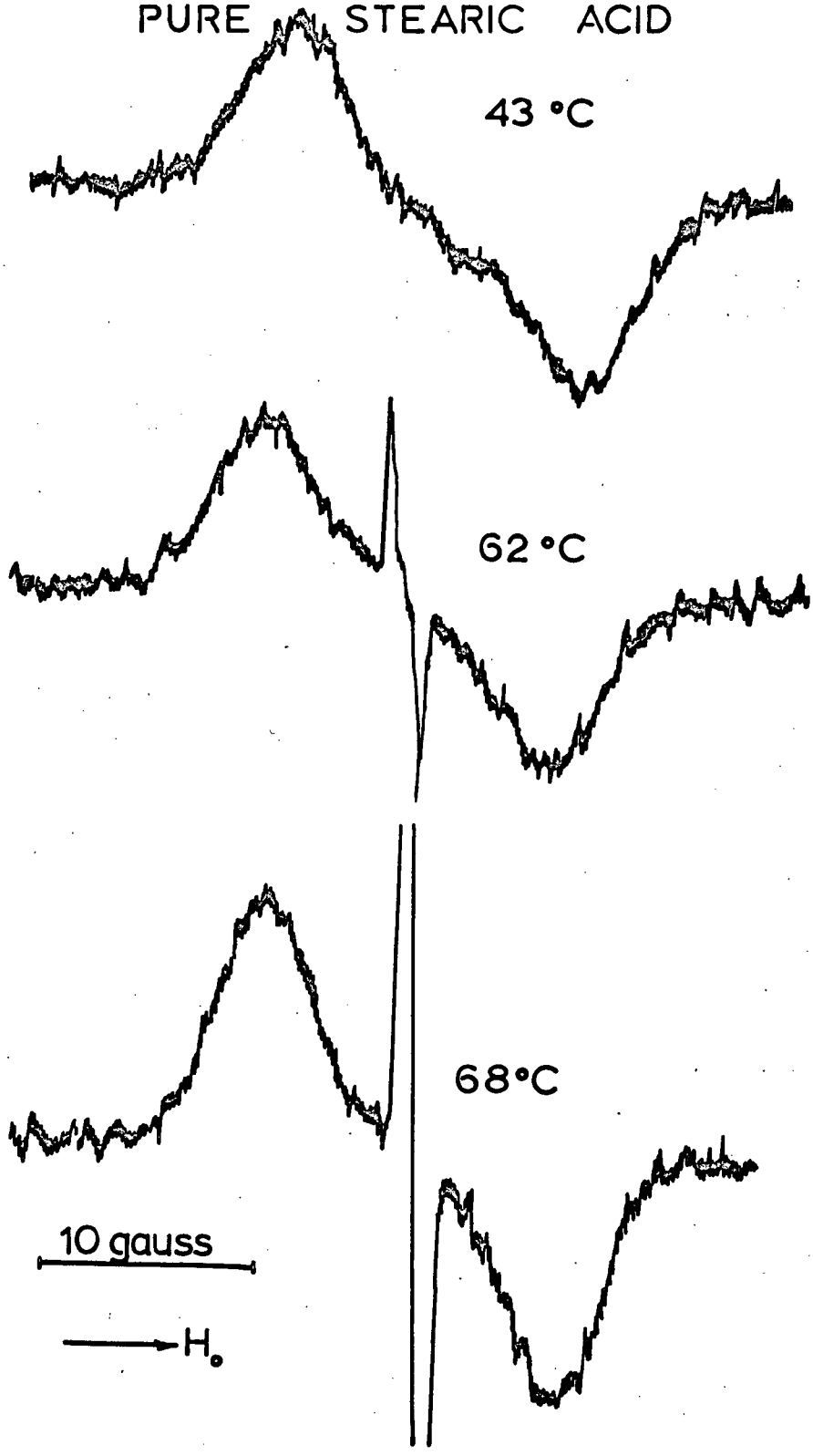

ments of Dunell[2] and Grant[1,2] indicate that the "average" liquid embryos should be greater than a certain limiting size. Frenkel[54] has derived the following quantitative expression for the fraction, J, of the sample molecules, N, contained within the liquid embryos:

$$J = \frac{1}{N} \sum_{g \geq g_o} g N_g = \frac{\int_{g_o}^{\infty} e^{-\beta g - \gamma g^{2/3}} g \, dg}{\int_{o}^{\infty} e^{-\beta g - \gamma g^{2/3}} g \, dg} \qquad (15)$$

where N_g is the number of liquid embryos containing g molecules, g_o is the minimum number of molecules that may be contained in a "stable" liquid embryo. The distribution of N_g is proportional to the exponential function containing β and γ where $\beta \cong \lambda(T_o - T)/(kT_o^2)$ when T, the temperature, lies sufficiently close to the transition or fusion temperature, T_o; λ is the heat of fusion per molecule in the embryo; and $\gamma = \mu/kT$, where μ is a function of the surface free energy or is approximately equal to $36\pi\sigma V_B^{2/3}$ where σ is the solid-liquid surface tension and $V_B^{2/3}$ is the surface area of the liquid embryo occupied by one molecule. σ is of the order one dyne/cm. V_B is about $1000A^3$. λ is approximately 14 kcal/mole for stearic acid. T_o is 69.3°C (342.5°K). A numerical integration of the above was shown to be very dependent on the choice of g_o. A numerical integration of the above equation, after choosing $g_o \sim 50$, did not reproduce the curves in Fig. 10 and 11. The calculated curve had a different shape from the observed curves, i.e. the calculated curve showed negligible premelting at $(T_o - T) > 0.5°$. It is significant that Francis, Piper, and Malkin[43] observe that the melting point of the acids, particularly those of high molecular weight, are not entirely independent of the treatment to which they are subjected during the process of purification. They also note that the melting point of the finely powdered crystals of an acid is higher than that of the bulk acid. In Fig. 10, one can see, for pure stearic acid, that thermal history is very

FIG. 10

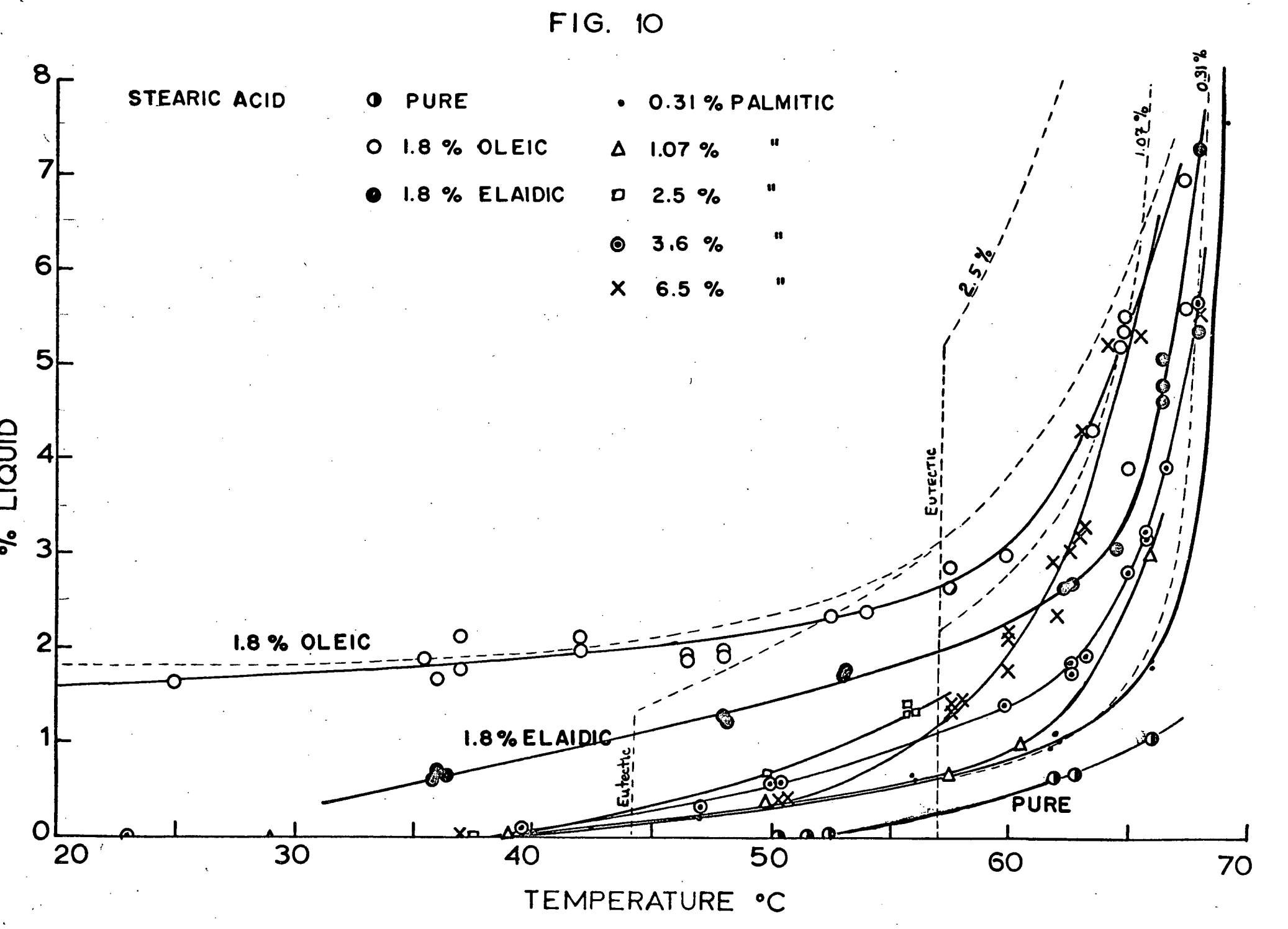
STEARIC ACID
PURE
1.8 % OLEIC
1.8 % ELAIDIC
0.31 % PALMITIC
1.07 %
2.5 %
3.6 %
6.5 %
"
% LIQUID
TEMPERATURE °C
0
1
2
3
4
5
6
7
8
20
30
40
50
60
70
1.8 % OLEIC
1.8 % ELAIDIC
PURE
Eutectic
Eutectic
2.5%
1.07%
0.31%

important in determining the amount of premelting observed in the stearic acid. Curves 1 and 2 of Fig. 11 were obtained for two different samples of pure stearic acid which were unfused but which had been annealed at 68°C. Curves 3 was obtained for acid which had been fused and annealed at 68°C and curve 4 was obtained for acid which had been fused but not annealed. It appears that a sample of crystalline stearic acid obtained from the melt is less perfect, i.e., free from defects, than the sample obtained from a saturated acetone solution although the latter is probably less pure than former due to occlusion of solvent molecules in the lattice on crystallization. It is significant that very little or no hysteresis was observed in the measurements, provided the sample was not fused in the process of measuring.

S. J. Lukasik[55] applied Frenkel's equation, (16), to heterophase fluctuations above the freezing point with limited success. Like Hoyer and Nolle[56], Lukasik writes that there was considerable difficulty in selecting values of g_o and σ .

Ubbelohde[57] uses a different definition for heterophase premelting. This, he defines, arises from a small mole fraction, n/N, of impurity when this is not soluble in the crystal but is soluble in the melt. He writes that the excess ΔQ of volume or of heat content change, which arises from actual formation of small amounts of liquid at a temperature T below the melting temperature T_o, is related to the total change ΔQ_o by the equation

$$\frac{\Delta Q}{\Delta Q_o} = \frac{nK}{N(T_o-T)} \qquad (17)$$

where K is the cryoscopic constant.

If "a" melting molecules each contribute a certain quantity of heat, q, to ΔQ then $\Delta Q = aq$. The number of liquid like molecules, A, at temperature T, is then:

$$A_T = \int_o^T \frac{nK}{(T_o-T)}\, dT = -nk \ln(T_o-T) \qquad (18)$$

FIG. 11

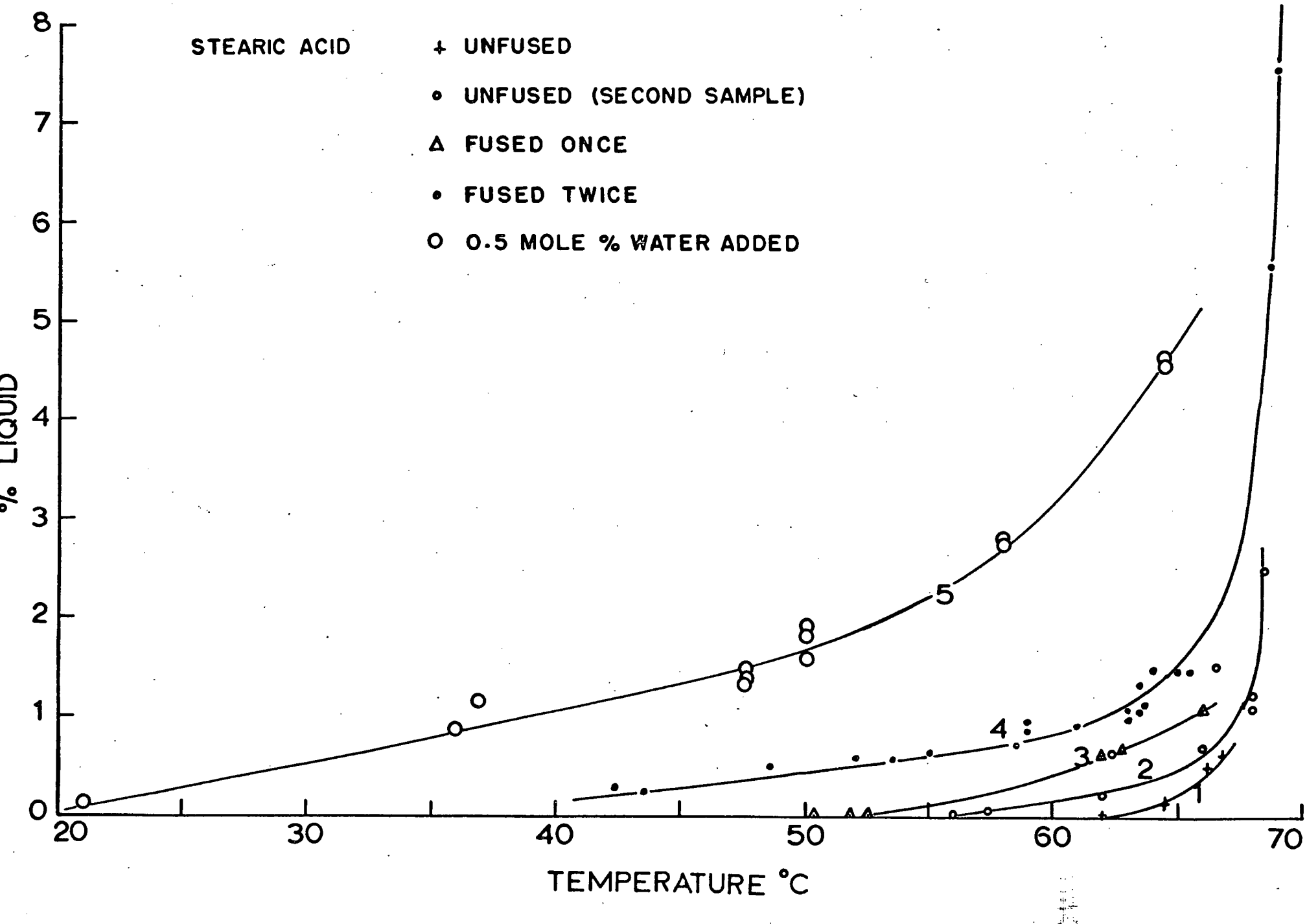
STEARIC ACID
+ UNFUSED
o UNFUSED (SECOND SAMPLE)
Δ FUSED ONCE
• FUSED TWICE
O 0.5 MOLE % WATER ADDED
% LIQUID
TEMPERATURE °C
0
1
2
3
4
5
6
7
8
20
30
40
50
60
70

A_T is proportional to the percentage of liquid as plotted in Figs. 11 and 12. Also A_T is proportional to $\ln(T_o-T)$ by (18). Inspection of (18) shows that A_T is not finite at $T = T_o$. It is not clear how Ubbelohde arrives at equation (17) and so it is difficult to emplain how one should account for A_T in (18), especially when $T = T_o$. It is obvious that A_T must be finite. Perhaps one may conclude that there is no sound basis for Ubbelohde's equation (16) and that it is empirical in origin, applying well to a particular experiment over a limited temperature range.

Francis, Collins and Piper[58] write that stearic and palmitic acids form a binary compound and that the phase diagram has eutectics at 27 and 52 per cent stearic acid. Similarly, elaidic and oleic acids have eutetics with stearic acid at seven and two per cent stearic acid, respectively. A plot of the percent liquid, as determined by application of the "lever-law" to the phase diagrams, shown in Fig. 12, is shown by the dotted lines in Fig. 6. The vertical lines (dotted) are drawn at the eutectic temperature, below which, presumably, the sample is solid. The correspondence of the observed and calculated per cent liquids may or may not be coincidental. It is not known whether palmitic acid forms a solid solution with stearic acid at certain concentrations. The percent liquid versus temperature curves (Fig. 10) continue without significant change in character far below the eutectic temperature. It is significant that the palmitic acid per cent liquid curves decrease to zero at the same temperature, ca. 39°C, at least 18° below the eutectic temperature. Perhaps there is a correlation here with pure fused stearic acid, which also shows a decrease to zero in the liquid like behaviour at circa 51°C, about 18°C below the melting point, although it is not clear why any correlation should exist.

One conclusion which may be drawn from the results, however, is that larger amounts of impurity have greater effects on the degree of crystallinity

FIG. 12

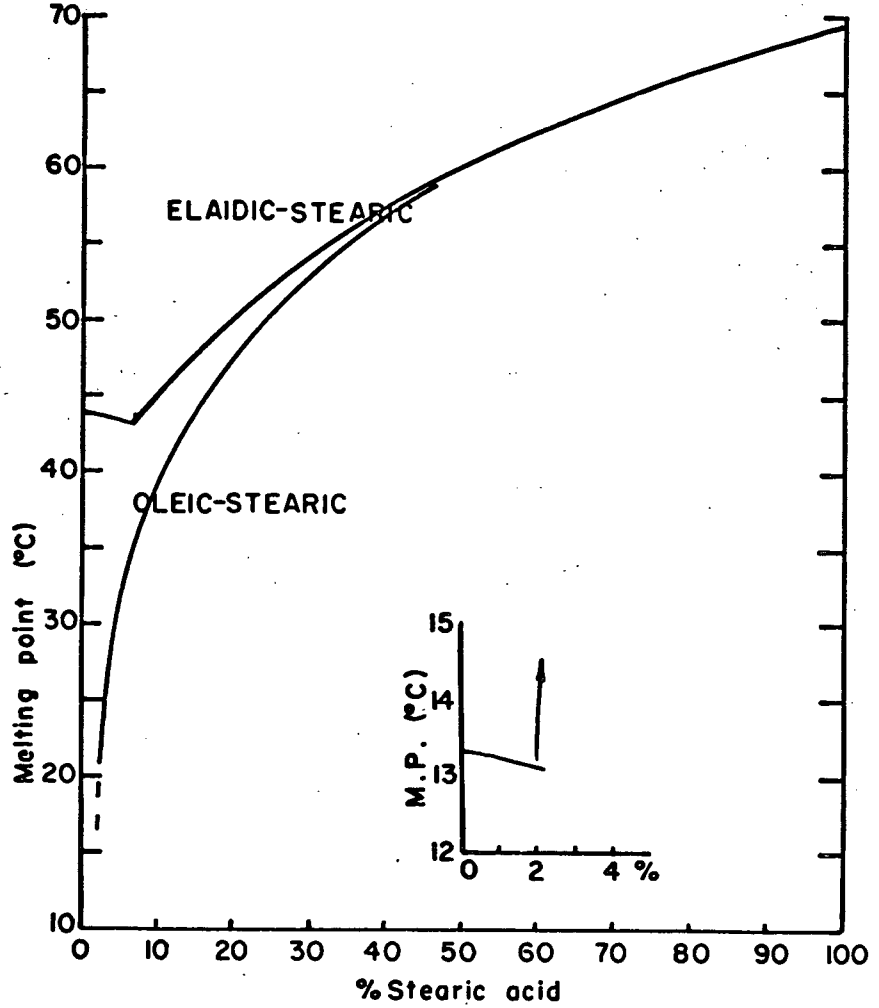
ELAIDIC-STEARIC
OLEIC-STEARIC
Melting point (°C)
% Stearic acid
M.P. (°C)
0 2 4 %

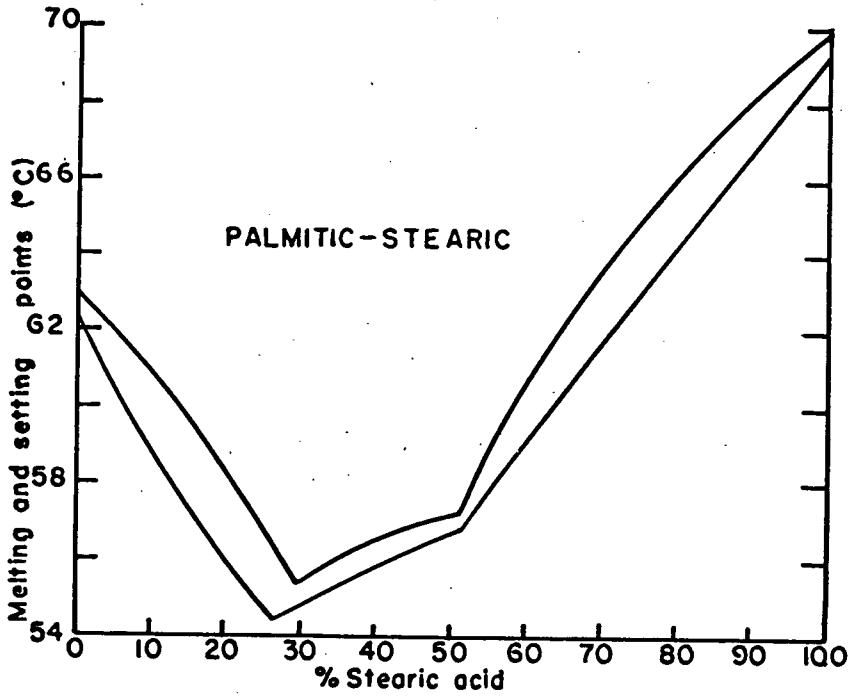
PALMITIC-STEARIC
Melting and setting points (°C)
% Stearic acid

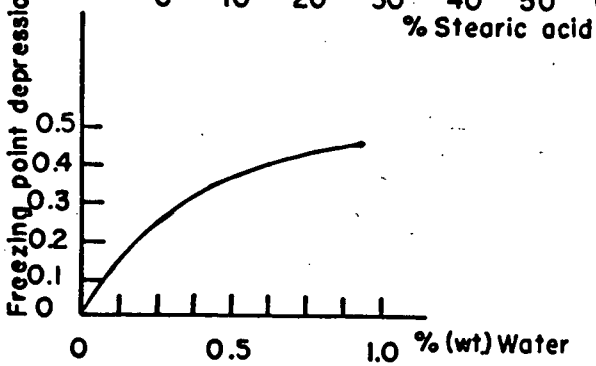
Freezing point depression (C°)
% (wt) Water

of the sample and that the effect may not be directly proportional to the amount of impurity present. This conclusion is not at all startling, especially if one looks again at Fig. 12.

It was expected that elaidic acid should have less effect on the premelting phenomenon than oleic acid due to the trans-arrangement of the paraffin chain about the olefinic C9 - C10 bond rather than the cis arrangement as found in oleic acid. One might say that elaidic acid is more like stearic acid than oleic acid. The effect of impurity on the fusion temperature is made evident by considering the entropy change during the transition. The heat of fusion, ΔH_f, is related to the change in entropy during the transition by the following relation:

$$\Delta H_f = T_f \Delta S_f$$

If impurities are localized at scattered sites throughout the lattice at $T < T_f$, then ΔS_f will be increased in magnitude. Similarly, T_f should decrease since ΔH_f is essentially constant. Significant results might be obtained if one were to measure the heat capacity (at constant pressure) over a temperature range, say $0^{\circ}C$ to $70^{\circ}C$ as a function of thermal history and impurity content of a stearic acid sample.

SPIN-LATTICE RELAXATION TIME, T_1, MEASUREMENTS.

Studies of the motional narrowing of the absorption are most useful in determining the types of motions occurring. Semiquantitative information regarding the rate of motion is achieved by analyzing the temperature dependence of the line width and second moment of the absorption signal, especially in the regions of rapid change. The spin lattice relaxation time, T_1, measurements supplement the broadline measurements by providing more direct and detailed information about the lattice motions over wide temperature ranges extending knowledge of molecular motions to temperatures above the fusion temperature. In stearic acid, the proton T_1 is governed by the thermal motions of the lattice,

which produce fluctuations in the local magnetic dipole fields. For solid stearic acid, it appears reasonable that the molecular torsional oscillations or reorientations will provide more effective relaxation than translational motions[59]. Neglecting the contribution of the latter, the T_1 for a given proton is given by equation (7).

Although one might expect different T_1 values for portons in different structural groups experimental results[59,60,61] indicate that the T_1's of the different protons are effectively equal. Equation(7) may be rewritten:

$$\frac{1}{T_1} = K \gamma^4 \hbar^2 \sum_{i>j} r_{ij}^{-6} \left[\frac{\tau}{1+(\omega\tau)^2} + \frac{4\tau}{1+(2\omega\tau)^2} \right] \qquad (19)$$

where K is a constant that depends on the geometry of the motional process (for example, reorientation about a single axis). If there is only one significant relaxation mechanism with a single correlation time, τ, corresponding to a thermal process with a potential barrier or activation energy, ΔE, then we have

$$\tau = \tau_\infty \exp(+\Delta E/RT)$$

In the limiting cases of $\omega\tau \ll 1$ and $\omega\tau \gg 1$, $1/T_1$ is directly proportional to τ and $1/\tau$, respectively. A plot of log T_1 versus $1/T$ should have two straight-line segments with slopes of $-\Delta E/2.303R$ and $\Delta E/2.303R$ for the high and low temperature regions, respectively. The constant K of equation (19) has the value 0.225 for three fold reorientation of the methyl group[60,62]. Consequently, the magnitude of $1/T_1$ at the T_1 minimum is given by [62] $0.321 (\gamma^4\hbar^2/\omega) \sum_{i>j} r_{ij}^{-6}$. Using 1.79 A as the interproton distance in the methyl group, the mimimum value of 0.055 seconds is calculated for an irradiation frequency of 16 Mc/sec. The experimental value (Fig. 13) of 0.052 seconds agrees with this quantity very well. The dotted curve in Fig. 14 was drawn using the Eq. (19) and assuming that the correlation time could be described using the values ΔE = 2.2 kcal/mole, $\tau_\infty = 1.585 \times 10^{-12}$ sec. τ at 77°K is

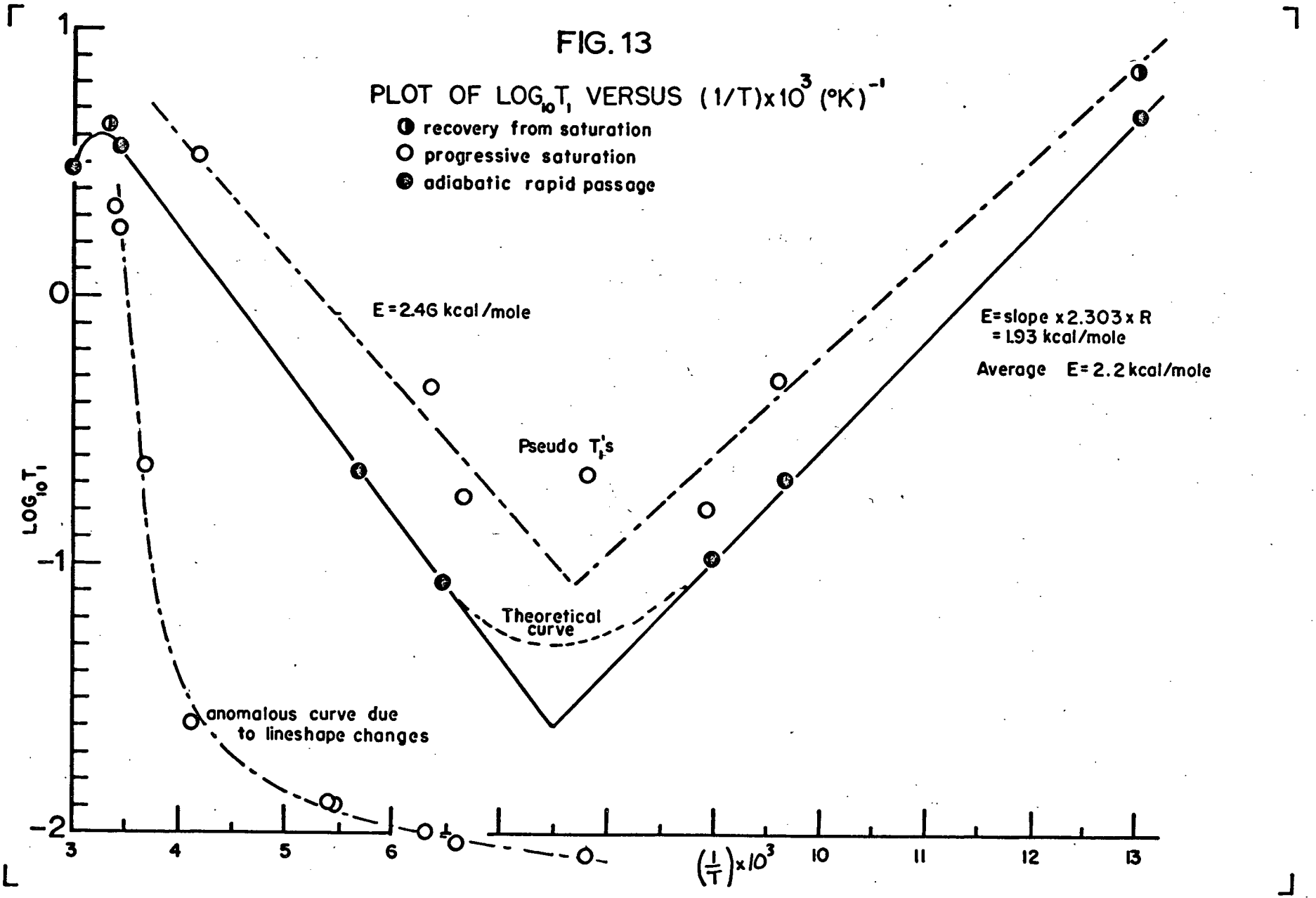
FIG. 13
PLOT OF LOG10T1 VERSUS (1/T)x10^3 (°K)^-1
recovery from saturation
progressive saturation
adiabatic rapid passage
E = 2.46 kcal/mole
E = slope x 2.303 x R
= 1.93 kcal/mole
Average E = 2.2 kcal/mole
Pseudo T1's
Theoretical curve
anomalous curve due to lineshape changes
LOG10T1
(1/T)x10^3
1
0
-1
-2
3
4
5
6
10
11
12
13

2.7×10^{-6} sec. The close agreement of experiment (the solid line in Fig. 13) with theory lends support to the postulate of Grant[1] and Dunell[1,2] that methyl group reorientation is occurring at a sufficiently high frequency to cause significant reduction in the second moment. The solid line in Fig. 13 is drawn through the T_1 values obtained from the adiabatic rapid passage results. The recovery from saturation T_1 results at 293°K and 77°K are, as expected, longer than the adiabatic rapid passage results. This is explained by considering the intensity of the observing r.f. field, H_1, in the recovery from saturation experiment. The observing r.f. field is of sufficient intensity to "slow down" the recovery by re-exciting the nuclear spins to the higher Zeeman energy levels. As a consequence of this inaccuracy in the T_1 measurement, the progressive saturation T_1 values are also longer since they are based on the T_1 value obtained from the recovery from saturation experiment used as a calibration. Changes in the absorption line shape in the presence of a saturating r.f. field introduces significant error in the progressive saturation T_1 measurements. As shown in Fig. 14, the plot of the signal amplitude versus r.f. field meter reading shows a "shoulder" as well as the expected maximum. In the manner of Wilson and Pake[63], the T_1 values were determined for the "shoulder" (taken as a maximum of a component signal of the absorption signal (Fig.14)) as well as for the actual maximum. These "shoulder" T_1's are labelled "pseudo T_1's" in Fig. 14. More accuracy in the progressive saturation measurements might have been acheived if a plot of integrated intensity of the absorption signal, instead of its derivative maximum, had been used. (This was not done since the time required to do this, about one day per single T_1 measurement, was prohibitive). It is certain that the modulation frequency, $2\pi\omega_m$= 80 cps, influences the line shape and hence the T_1 values obtained[36,37,68].

FIG. 14

GRAPH SHOWING DEPENDENCE OF SIGNAL AMPLITUDE ON R.F. FIELD INTENSITY

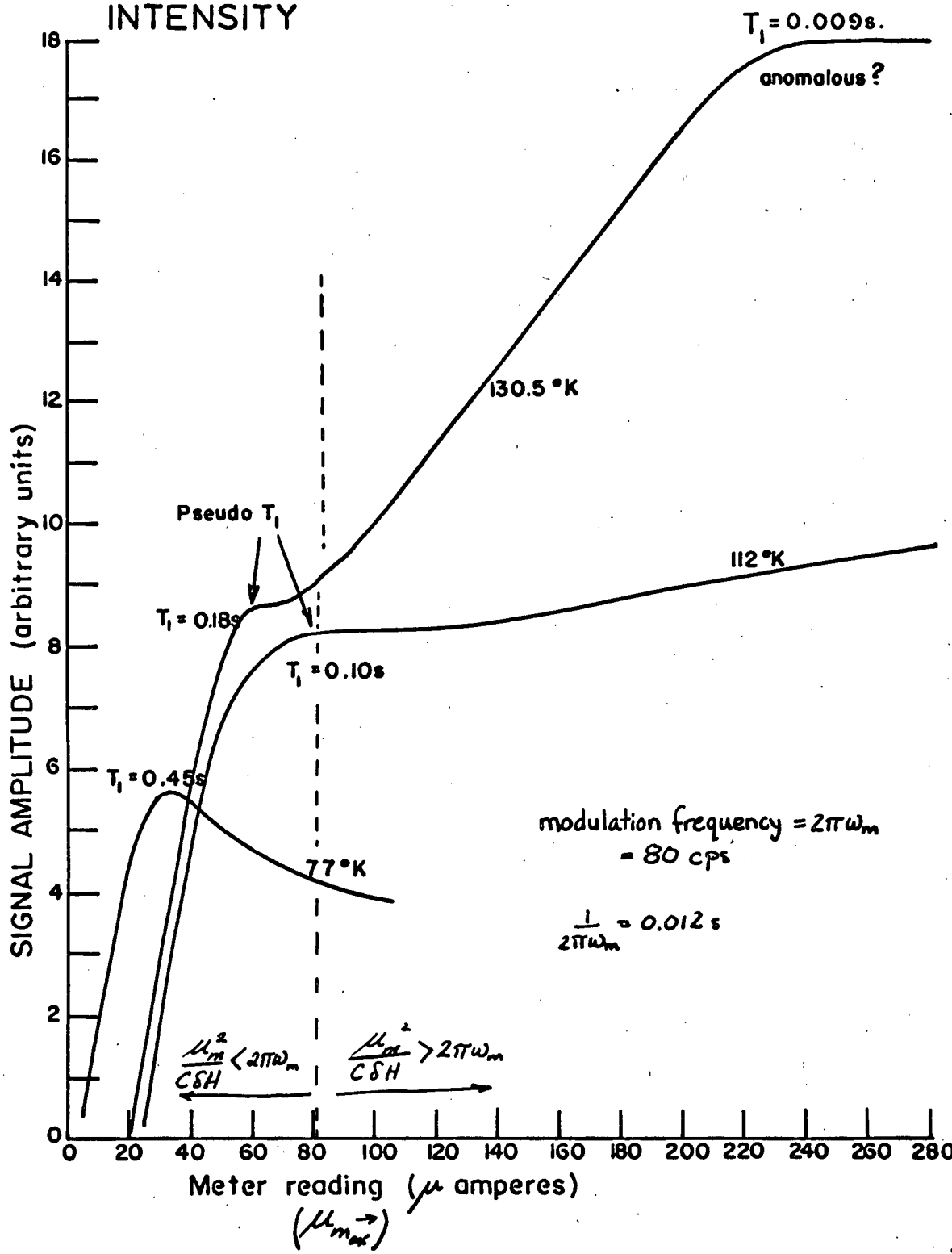

The adiabatic conditions cited in the experimental section of this thesis as Eq. (13) are:

$$\frac{\delta H}{T_1} \ll \frac{dH_0}{dt} < \gamma H_1 \delta H \tag{13}$$

These conditions were derived in the course of the writing of this thesis in an attempt to explain why the adiabatic rapid passage experiment was possible at all for solids. Abragam[64] writes that the requirements derived by Bloch[65] for the adiabatic rapid passage experiment

$$\frac{H_1}{T_2} \ll \frac{dH_0}{dt} \ll \gamma H_1^2 \tag{20}$$

are unreasonable when extended to solids, where T_2 is of the order 10^{-5} seconds. Abragam rewrites (20) in the form:

$$\frac{1}{T_1} \ll \frac{1}{H_1} \quad \frac{dH_0}{dt} \ll \gamma H_1 \sim \frac{1}{T_2} \tag{21}$$

The first condition of (21) may be restated: the time of passage through resonance must be short compared to T_1. Abragam has assumed that H_1 is larger than the line-width δH. In practice, we find that a value of $H_1 = 15$ gauss is very difficult to achieve, due to experimental limitations. The time of passage through resonance, if $H_1 < \delta H$, is

$$\left[\frac{1}{\delta H}\frac{dH_0}{dt}\right]^{-1}$$

The final condition of (21)

$$\frac{dH_0}{dt} \ll \gamma H_1^2 \tag{22}$$

is derived by Abragam for vaues of $H_1 \gtrsim \delta H$. The origin of the condition (22) is readily seen by considering the following physical picture of the adiabatic rapid passage experiment.

Consider an applied field $(H_0(t), H_1 \cos\omega t, H_1 \sin\omega t)$. "Transform to a rotating coordinate system rotating at ω about OZ, so that the effective

field in the rotating coordinate system is $(H_0(t) = \omega/\gamma, H_1, 0)$. We need now only consider the precession about the resultant field, $\vec{H}_{eff}(t)$. As we pass through resonance, i.e. $H_0(t) = \omega_0/\gamma$, the field component $H_0(t) = \omega/\gamma$ changes sign and similarly $\vec{H}_{eff}$ changes its sense from positive to negative. As we pass through resonance in a time very short compared to T_1, T_2 i.e. $\delta H/(dH_0/dt) \ll T_1, T_2$, $\vec{H}_{eff}$ begins to rotate and tends to leave $\vec{M}$, the magnetization, behind. However, as soon as this happens, $\vec{M}$ begins to precess about $\vec{H}_{eff}$ but the angle between $\vec{M}$ and $\vec{H}_{eff}$ never gets very big because, as $\vec{M}$ gets left behind $\vec{H}_{eff}$, the precession tends to swing the magnetization round, provided there is time for this to happen. Thus the magnetization $\vec{M}$ follows $\vec{H}_{eff}$, which after the passage through resonance, is in the negative OZ direction. Reverting to the laboratory frame does not affect this magnetization which is therefore found to be reversed[40].

This signal observed during a passage corresponds to a transverse magnetization, which is, collinear with H_1, and which under the right conditions is equal to the magnetization vector M[64]. At the end of this passage $M_z = -M_0$ and t seconds later it is $M_z = M_0(1 - 2e^{-t}/T_1)$. The signal of the second fast passage going back through the resonance is proportional to $-M_z$. The negative sign is due to the fact that the first and second signals are observed starting from opposite sides of the resonance. For a symmetrical sweep, where the time, t, between sweeps through resonance is the same for opposite directions and where the sweep amplitude is small compared to the external magnetic field, $H_0(t)$, a steady state value of M_z, the nuclear magnetization, is given by (Eq. (14)):

$$M = M_0 \quad \frac{(1 - \exp(-t/T_1))}{(1 + \exp(-t/T_1))} \qquad (14)$$

Since, according to Abragam, the signal height of the rapid passage signal is proportional to M, it is possible, as shown in the experimental section

of this thesis, to measure T_1 in terms of Eq. (15). The T_2 requirement in Eq.(20) is important since the transverse magnetization decays to zero in a time of the order of T_2[64]. In a solid, T_2 is of the order 10^{-5} seconds. This implies that the time of passage through resonance must be short compared to 10^{-5} seconds. For a line-width of ca. 15 gauss, this requirement states that we must sweep the field at a rate greater than 15×10^5 gauss per second! The condition (21) derived by Abragam, requires that the time of passage through resonance is long compared to T_2. He does not explain the origin of the " $\approx$ ", on the right hand side of (21). He shows that the transverse magnetization will reach irreversibly an equilibrium value $M_0 H_1^2/(H_1^2 + \delta H^2)$. Once this value is reached, any further decrease can only come from the spin-lattice relaxation time.

δH in the above relation is the usual line-width. Since $\delta H > H_1$, the maximum transverse magnetization obtainable by rapid passage is of the order of $M_0 H_1/\delta H$. Complications arise when line-shape changes arise in the presence of the strong r.f. field.

Powles[40] introduces a novel presentation of the derivation of the adiabatic rapid passage conditions. "Adiabatic, in the Ehrenfest sense, means that the change in the system during the perturbation is so slow that there is negligible change in the populations of the energy levels. This is manifestly not so in this experiment since we have a resonant perturbation and there is significant change in the populations of the levels. It is just that this gives the reversal of the magnetization. However, in the rotating coordinate system the perturbation becomes non-resonant and we may imagine we have energy levels determined by H_{eff}, i.e. the energy level separation ΔE is $\hbar\gamma H_{eff}$. Now for a non-resonant perturbation, the adiabatic condition

is simply [35] $\frac{1}{\tau} \ll \frac{\Delta E}{\hbar}$ where τ is the time of application of the perturbation and ΔE is the energy separation of the levels in question."[40] The τ in this case is evidently the time "at or near resonance", so that we require

$$\left(\frac{dH_0}{dt}\right) / \delta H \ll \gamma H_{eff}$$

and since the minimum value of H_{eff} is H_1 we require that

$$\left(\frac{dH_0}{dt}\right) \ll \gamma H_1 \delta H$$

as in (13). In a sense then, the populations remain unchanged (and so dies the entropy) but the energy levels are reversed and so is the magnetization.

The conditions (13) may be rewritten:

$$\frac{1}{T_1} \ll \frac{dH_0}{dt} / \delta H < \gamma H_1$$

Experimentally T_1 was greater than 0.08 seconds, $\delta H/(dH_0/dt)$ was 18×10^{-3} seconds and so the left hand side of (13) is satisfied. H_1 was normally 0.2 gauss and so $(\gamma H_1)^{-1}$ was approximately 0.0017 seconds, which is very much less than 18×10^{-3} seconds, the time spent passing through resonance. The conditions (13) were tested by first reducing (dH_0/dt) and then by reducing H_1. That the left side of (13) was necessary is indicated by the traces in Fig. 15b. H_1 was reduced by a factor of 10 without affecting the T_1 values. Only when H_1 was reduced by a factor of 25, did any significant changes in the oscilloscope trace (other than signal to noise ratio) become apparent. (Fig.15 c). Redfield[36] and Abragam both agree, however, that it is still necessary to use r.f. levels above the saturation level.

FIG. 15

OSCILLOSCOPE TRACINGS FROM ADIABATIC FAST PASSAGE EXPERIMENT

(a) Satisfying (13)

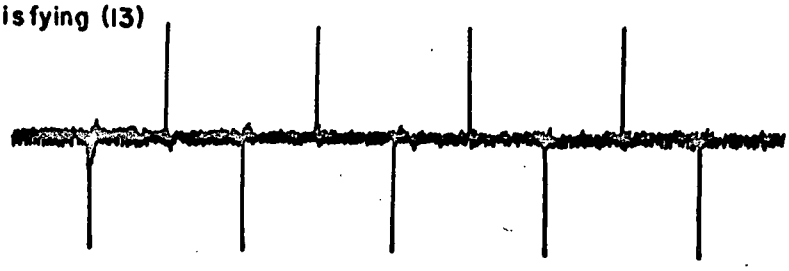

(b) (dH_0/dt) to small

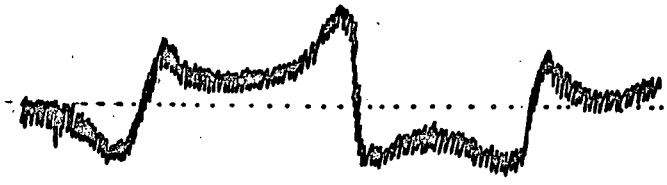

(c) H_1 too small

SUMMARY

The proton magnetic resonance absorption of the C-form of stearic acid has been studied over the temperature range 77°K to 342.5°K.

The broadline measurements do not indicate what types of motion are occurring in the solid stearic acid at low temperatures. The appearance of a narrow component on the usual broadline spectrum at temperatures greater than room temperature is interpreted to be caused by large liquid regions in the lattice. The number and size of these defects increases with increase in temperature and with the incorporation of various types of defects in the solid lattice. It has been shown that impurities more "unlike" stearic acid increase the amount of liquid-like motion present in the lattice. Oleic acid (cis olefin) causes more premelting than elaidic acid (trans olefin), which is more "like" stearic acid. Increasing amounts of palmitic acid impurity give increasing amounts of premelting. Various theories have been tested, without success, to explain the premelting phenomenon.

Spin-lattice relaxation times, T_1, were measured by adiabatic rapid passage. The results indicate that the principal Zeeman energy-thermal bath coupling occurs through methyl group reorientations. An activation energy of 2.2 kcalories/mole for methyl group rotation about the C3 axis in solid stearic acid and a rotation frequency of 4×10^5 sec^{-1} at 77°K were determined from the T_1 data. The experimental T_1 results agree well with theory.

APPENDIX A.

Computation of the Area or Integrated Intensity of the Absorption Signal.

If the line shape function is a continuous function, g(H), where the resonance centre is at H = 0, then;

$$\text{Area} = \int_{-\infty}^{\infty} g(H)\, dH = H\, g(H)\Big|_{-\infty}^{\infty} - \int_{-\infty}^{\infty} g'(H)\, H\, dH \qquad (1)$$

However, the first term above is equal to zero at the limits $\pm\infty$. The problem, then, is the evaluation of the second term.

$$\text{Area} = -\int_{-\infty}^{\infty} g'(H)\, H\, dH \qquad (2)$$

The line shape function, g(H), is symmetric about the centre of resonance. If g'(H) is a slowly verying function, continuous at all H, (2) may be replaced by the summation:

$$\text{Area} = -2\delta^2 \sum_{n=1}^{\infty} g'(n)\, n \qquad (3)$$

where (3) is the summation of the product of the magnitude of the derivative curve and the distance from the centre of resonance, n increments each of magnitude δ.

The line shape function for the narrow component is assumed to be a step function of the type;

$$g'(H) = \frac{g'(h_m)}{h_m} \times H \qquad -h_m \leqslant H \leqslant h_m$$

$$g'(H) = 0 \qquad |H| > h_m$$

where 2 $g(h_m)$ is the peak to Peak amplitude and h_m is the modulation amplitude.

Substituting this into (1) one has;

$$\text{Area} = \frac{g(H)}{h_m} \times \frac{H^3}{2}\Big|_{-h_m}^{h_m} - \int_{-h_m}^{h_m} \frac{g(H)}{h_m} H^2\, dH$$

$$= 0 - \frac{2}{3} g'(h_m) h_m^2$$

$$= -2/3\, g'(h_m) h_m^2 \qquad (4)$$

The summation (3) is made sufficiently accurate by limiting the magnitude of δ. In practice it was found that δ could be made as large as on fifteenth the line-width without significantly affecting the calculated area. Corrections for modulation broadening are assumed to be nonexistent here, since line broadening presumably does not change the integrated intensity of the signal.

APPENDIX B.

Computer program for calculation of relative integrated Intensity of the Narrow and Broad Component.

The relative integrated intensities of the two components were determined by numerical evaluation of equations (3) and (4) of Appendix A. The spectra were measured as indicated in Fig. 16. The fraction of molecules undergoing liquid-like motion, J, is then:

$$J = 2/3\ g'(h_m)\ h_m^2/(2\delta^2 \sum_n n\ g(n) + 2/3\ g'(h_m)\ h_m^2)$$

The fortran IV program was as follows:

```
      DIMENSION NG1 (50), NG2(50), TITLE(10)
6     READ (5,1) NMAXI, NMAX2, HM, GHM, DELTA, (TITLE(I),I = 1,10)
      READ (5,2) (NG2(I), I = 1,NMAX2)
      LIQF = 0.66667*GHM*HM*HM
      N1 = 0
      DO 4 I = 1,NMAX1
4     N1 = N1 + I*NG1(I)
      DO 5 I = 1,NMAX2
5     N1 = N1 + I*NG2(I)
      LIQF = LIQF/(2.*DELTA*DELTA*FLOAT(N1) + LIQF)
      WRITE(6,3) LIQF,(TITLE(I),I = 1,10)
1     FORMAT (2I2,F6.4, F4.0,F7.5,9A6,A5)
2     FORMAT (26I3,2X)
3     FORMAT (1X,17HLIQUID FRACTION =, F6.4,L)X,10A6)
      GO TO 6
      END
```

The experimental second moments programme was a slight alternation to this programme in that the summation is:

$$SM = 1/3\ S^2\ \frac{\sum n^3\ g'(n)}{\sum n\ g'(n)} - \frac{h_m^2}{4}$$

FIG. 16

A TYPICAL DERIVATIVE CURVE FOR STEARIC ACID

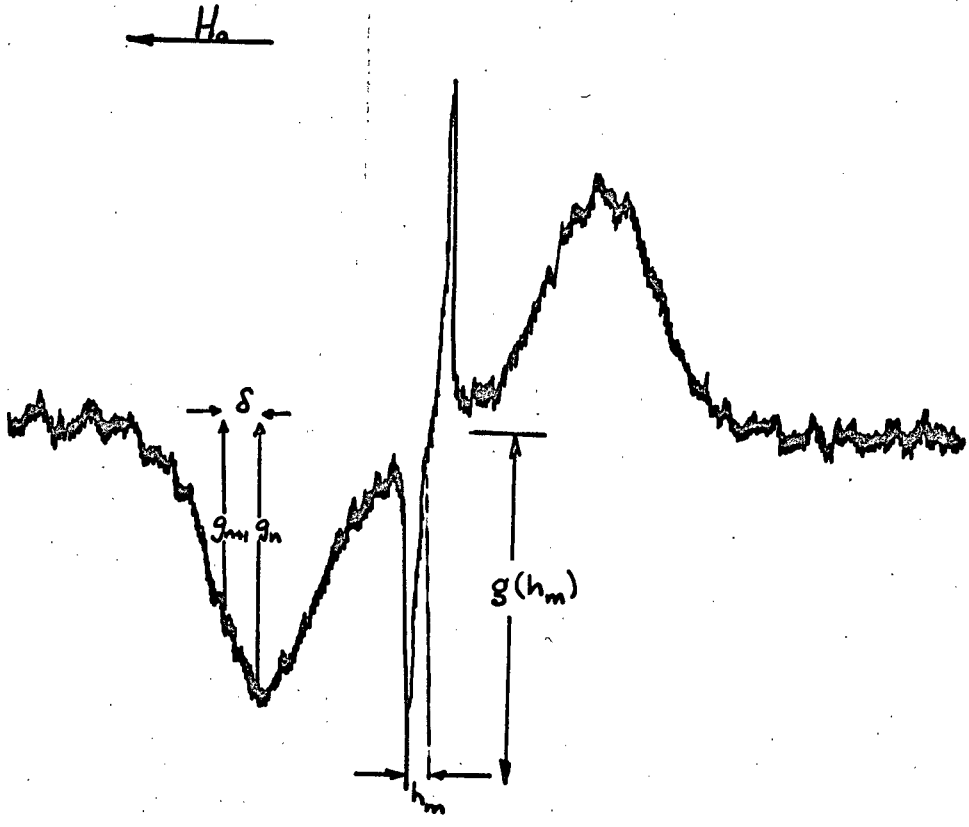

line width δH = 13.6 gauss

Two theoretical second moment programmes were written, one which calculated the rigid lattice second moment (e.g., on page 10) and the other which evaluated the second moment for various types of motion. The latter summed the terms

$$716.22 \sum_{i>j} \frac{\rho_1 \rho_2}{r_{ij}^6} = SM$$

where ρ_1 and ρ_2 are defined in equations (3) and (4) on page 11 of this thesis. It is questionable whether one can legitimately utilise the product $\rho_1 * \rho_2$ in the summation since the effects of the motions ρ_1 and ρ_2 are not entirely independent.

BIBLIOGRAPHY

1. R.F. Grant and B.A. Dunell, Can. J Chem. 38, 359 (1960)

2. R.F. Grant, thesis, U.B.C. (1960)

3. E. Stenhagen and E. von Sydow, Arkiv. Kemi. 6, 309 (1953)

4. W.S. Singleton, T.L. Ward, and F.G. Dollear, J.A. Oil Chem. Soc. (1950) p.143.

5. N. Adriaanse, H. Dekker and J. Coops, Rec. Trav. Chem. 84, 393 (1965); 83, 557(1964).

6. E. von Sydow, Arkiv. Kemi. 9, 231 (1956).

7. K.S. Markley, "Fatty Acids", Interscience Pub., N.Y.,(1947) p.222.

8. M.R. Barr, B.A. Dunell, and R.F. Grant, Can.J. Chem. 41, 1188(1963).

9. G.W. Gray, "Molecular Structure and the Properties of Liquid Crystals", Academic Press, N.Y., 1962 p. 148.

10. N.V. Sidgwick, Ann. Reports Chem. Soc., 30, 115(1931).

11. J.A. Dave and M.J.S. Dewar, J. Chem Soc. 4305(1955).

12. G.W. Gray, ref. 9,p.125.

13. G.H. Brown and W.G. Shaw, Chem. Rev. 57, 1049 (1957).

14. K.S. Markley, Ref. 7, p.226.

15. A. Muller, Trans. Farad. Soc. 29, 990 (1933).

16. A. Muller, Proc. Roy. Soc. 138A, 514 (1932).

17. R.W. Crowe and C.P. Smyth, J.A.C.S., 73, 5401 (1951).

18. A.K. Saha and T.P. Das, "Theory and Applications of Nuclear Induction", Calcutta, India (1957) p.292.

19. E.R. Andrew, "Nuclear Magnetic Resonance", Cambridge Univ. Press, 1958, Ch.5.

20. A. Abragam, "The Principles of Nuclear Magnetism", Clarendon Press, Oxford, 1961 p. 324-326.

21. J.H. van Vleck, Phys. Rev. 74, 1168 (1948).

22. E.R. Andrew and R.G. Eades, Proc. Roy. Soc., A218, 537 (1953).

23. LV. Dmitrieva and V.V. Moskalev, Sov. Phys. Solid State, 5, 1623(1964).

24. V.V. Moskalev, Sov. Phys. Solid State, 3, 2218 (1962).

25. H.S. Gutowsky and G.E. Pake, J. Chem. Phys., 18, 162 (1950)

26. A. Abragam, ref. 19, p.434 (equation 24), also see p.452-479 for a general discussion concerning equations (3) and (4) and other types of motion in the lattice.

27. A. Abragam, ref. 20, p.542.

28. N. Bloembergen, E.M. Purcell, and R.V. Pound, Phys. Rev., 73, 679 (1948).

29. R. Kubo and K. Tomita, J. Phys. Soc. (Japan), 9, 888 (1954).

30. G.W. Smith, General Motors Research Publication, G.M. R. - 457, January, 1965.

31. T. Yukitoshi, H. Suga, S. Seki and J. Itoh, J. Phys. Soc. Japan, 12, 506 (1957).

32. S. Linder, J. Chem Phys., 26, 900 (1957).

33. D.W. McCall and D.C. Douglass, J. Chem. Phys., 33, 777 (1960).

34. G.W. Smith, J. Chem. Phys. 36, 3081 (1962).

35. D. Bohm, "Quantum Theory". Prentice-Hall Inc., N.J., (1951) p.449.

36. A.G. Redfield, Phys. Rev. 98, 1787 (1955).

37. M. Goldman, J. Physique, 25, 843 (1964).

38. L.E. Drain, Proc. Phys. Soc., A62, 301 (1949).

39. G. Chiarotti, G. Cristiani and L. Giulotto, Nuovo Cimento, 1, 863 (1955):

40. J.G. Powles, Proc. Phys. Soc. (London), 71, 497 (1958).

41. W.A. Anderson, "N.M.R. and E.P.R. Spectroscopy, Varian 3rd Annual Workshop", Pergamon Press, N.Y., (1960) p.164.

42. J.B. Brown and D.K. Kolb, "Progress in the chemistry of fats and other Lipids". Pergammon Press, Ltd., London, Vol.3, (1955) p.58.

43. F. Francis, S.H. Piper and T. Malkin, Proc. Roy. Soc. (London) A128, 214 (1930).

44. The Hormel Institute, Austin, Minnesota.

45. E.R. Andrew, J. Chem Phys., 18, 607 (1950).

46. R.W. Crowe and C.P. Smyth, J.A.C.S. 73, 5401 (1951).

47. H.S. Gutowsky, G.E. Pake, and R. Bersohn, J. Chem. Phys., 22, 643 (1954).

48. B. Pederson, "N.M.R. in Hydrate Crystals: Correction for Vibrational Motion", preprint to publication in J. Chem. Phys. 1965.

49. J.A. Ibers and D.P. Stevenson, J. Chem. Phys., 28, 929 (1958).

50. F.A. Rushworth, Proc. Roy. Soc. A222, 526 (1954).

51. V. Vand, W.M. Morley and T.R.Lomer, Acta Cryst. 4, 324 (1951).

52. A. Muller, Proc. Roy. Soc. (London), A154, 624 (1936).

53. K. Illers, Rheologica Acta, 3(4), 185, 194 (1964).

54. J. Frenkel, "Kinetic Theory of Liquids", Clarendon Press (Oxford), 1946, p.388.

55. S.J. Lukasik, J. Chem. Phys. 27, 523 (1957).

56. W.A. Hoyer and A.W. Nolle, J.Chem. Phys., 24, 803 (1956).

57. A.R. Ubbelohde, Pure and Appl. Chem., 2, 251 (1961).

58. F. Francis, F.J.E. Collins, and S.H. Piper, Proc. Roy. Soc.(London) A158, 691 (1937).

59. H.S. Gutowsky, A. Saike, M. Takeda, and E.D. Woessner, J. Chem. Phys., 27, 534 (1957).

60. E.O. Stejskal, D.E. Woessner, T.C. Farrar, and H.S. Gutowsky, J. Chem. Phys., 31, 55 (1959).

61. I. Solomon, Phys. Rev. 99, 559 (1955).

62. J.E. Anderson and W.P. Slichter, J. Chem. Phys., 41, 1922 (1964).

63. C.W. Wilson land G.E. Pake, J.Chem. Phys., 27, 115 (1957).

64. A. Abragam, ref. 20, p.66-67, 548-553.

65. F. Bloch, W.W. Hansen, and M. Packard, Phys. Rev., 70, 474 (1946).

66. N. Bloembergen: Thesis (Leiden, 1948).

67. J.G. Powles, Brit. J. Appl. Phys., 9, 277 (1958).

68. M. Lee, thesis, Pennsylvania State University (1964).